NASA Contractor Report 3913

The Design and Analysis of Simple Low Speed Flap Systems With the Aid of Linearized Theory Computer Programs

Harry W. Carlson

Date for general release ___ August 1987 ___

NASA

NASA Contractor Report 3913

The Design and Analysis of Simple Low Speed Flap Systems With the Aid of Linearized Theory Computer Programs

Harry W. Carlson

Kentron International, Incorporated
Hampton, Virginia

NASA

National Aeronautics
and Space Administration

**Scientific and Technical
Information Branch**

1985

INTRODUCTION

A linearized theory numerical method and a computer program for the aerodynamic design and analysis of wings with attainable thrust and vortex force considerations were introduced in reference 1 and further described in reference 2. A companion computer program which provides predictions of the low speed aerodynamic performance of wings with leading-edge and trailing-edge flaps is described in reference 3. The purpose of this report is to show how these two computer programs in combination may be used for the design of low speed wing flap systems capable of high levels of aerodynamic efficiency.

A fundamental premise of the study is that high levels of aerodynamic performance for flap systems can be achieved only if the flow about the wing remains predominantly attached. Or, in other words, it is assumed that attached flow performance levels can be approached provided that flow separation is relatively mild and is sufficiently localized. In accordance with this premise, the wing design computer program of reference 1 will be used to provide idealized linearized theory attached flow camber surfaces from which candidate flap surfaces may be derived. In a following step, the flap evaluation solution given by the computer program of reference 3 will be used to provide estimates of the aerodynamic performance of the candidate systems.

The design strategies and techniques that may be employed are illustrated through a series of examples. First the problem of designing flaps for wings with sharp leading edges which cannot achieve leading-edge thrust is treated, and then the influence of rounded leading edges which allow the development of leading-edge thrust is examined. The applicability of the numerical methods to the analysis of a representative flap system (although not a system designed by the process described herein) is demonstrated in a comparison with experimental data.

SYMBOLS

AR	wing aspect ratio, b^2/S
b	wing span
c	local wing chord
c_r	wing root chord
c_t	section theoretical leading-edge thrust coefficient
c_A	section axial or chord force coefficient
c_N	section normal force coefficient
C_A	wing axial or chord force coefficient
C_D	wing drag coefficient
ΔC_D	drag due to lift coefficient, $C_D - C_{D,\alpha=0}$ for the same wing with no camber or twist
C_L	wing lift coefficient
$C_{L,des}$	wing design lift coefficient
$C_{L,\alpha}$	wing lift curve slope at $\alpha=0$, per degree
$C_{m,des}$	wing design pitching moment coefficient
C_N	wing normal force coefficient
ΔC_p	lifting pressure coefficient
M	Mach number
r	wing section leading-edge radius
R	Reynolds number
S	wing reference area
S_s	suction parameter, $\dfrac{C_L \tan (C_L/C_{L,\alpha}) - \Delta C_D}{C_L \tan (C_L/C_{L,\alpha}) - C_L^2/(\pi AR)}$
t	wing section maximum thickness
x,y,z	Cartesian coordinates

x' distance in the x direction measured from the wing leading edge

α wing angle of attack, degrees

δ_L leading edge flap streamwise deflection angle, degrees, positive with leading edge down

$\delta_{L,n}$ leading-edge flap deflection angle measured normal to the hinge line, degrees, positive with leading edge down

δ_T trailing-edge flap streamwise deflection angle, degrees, positive with trailing edge down

$\delta_{T,n}$ trailing-edge flap deflection angle measured normal to the hinge line, degrees, positive with trailing edge down

$\delta_L factor$ leading-edge flap deflection multiplier

$\delta_T factor$ trailing-edge flap deflection multiplier

Λ wing leading-edge sweep angle, degrees

GENERAL PRINCIPLES

It is assumed that maximization of the aerodynamic performance of wings (minimization of drag-due-to-lift) can be achieved only through attached flow. For thick wings at high Reynolds numbers it may be possible as shown in sketch (a) to achieve attached flow without resorting to wing camber or twist. A large enough leading-edge radius will permit attached flow over the entire airfoil section and will

Sketch (a)

allow the development of full theoretical leading-edge thrust. For thin wings and low Reynolds numbers only well designed camber and twist, as shown in sketch (b), can be expected to permit attached flow. An airfoil section such as this can provide a distributed thrust over much of the forward portion of the airfoil which replaces the concentrated theoretical leading-edge thrust and leads to comparable

Sketch (b)

performance. Actually, even the best cambered and twisted surface cannot assure attached flow (especially at high lift coefficients) but for thin wings and low Reynolds numbers it offers the only possibility. Without camber and twist, a thin wing section would produce a separated flow, perhaps as that shown in sketch (c). If the
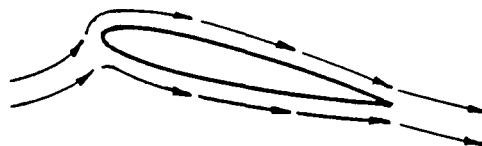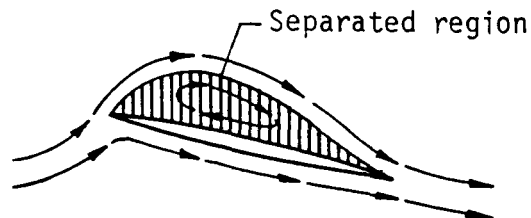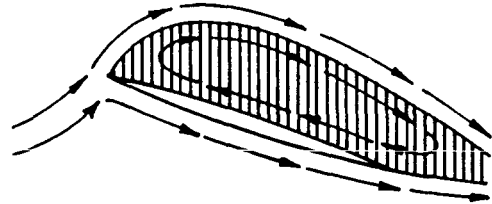
Sketch (c)

flow reattaches on the airfoil itself, the leading-edge thrust is not lost, but appears as a vortex normal force rather than a thrust force according to the Polhamus leading-edge suction analogy (reference 4). There is, however, a substantial loss in lifting efficien-cy. With more severe separation as shown in sketch (d) there would be a further loss in lifting efficiency. When the separated flow does not reattach on the airfoil itself, there is not only a loss of the vortex force

Sketch (d)

but also a reduced turning of the upper surface flow as depicted by the streamline above the separated region. Both of these effects bring about a loss in the normal force and an increase in drag for a given lift.

When the designer is not free to choose a continuously curved surface, but must rely on simple hinged flaps the goal of attached flow for thin wings may not be realistic. Certainly it is not achievable for reasonable flight conditions if design constraints call for a sharp leading edge. However, high levels of aerodynamic performance may still be reached if the flow is predominantly attached. Such a flow condition for a sharp leading edge wing is shown in sketch (e). Here the sharp leading edge triggers a separated flow which reattaches at the leading-edge flap hinge line. This condition meets one of the primary considerations in the design of "Vortex Flaps" as described in reference 5. This type of flow, with its limited and localized separation, may be said to be

Sketch (e)

predominantly attached. Note the similarity to the flow patterns depicted in sketch (b) for the cambered and twisted section with attached flow. For a thin wing with a rounded leading edge, the situation might not be much different except that, as shown in sketch (f), a somewhat smaller leading-edge flap deflection would result in a flow reattachment at the hinge line.
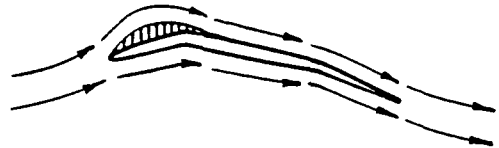
Sketch (f)

With a predominantly attached flow established as a flap system design goal, the attached flow camber and twist surface generated by the wing design program of reference 1 (or any other suitable design method) becomes a logical starting point. Camber surfaces given by the program can be used in the definition of candidate flap systems which approximate the surface slopes and the loadings of the wing design. Then a flap system analysis program, such as that of reference 3, can be used in estimating the aerodynamic potential of the candidate flap system and in design-by-iteration studies involving various flap geometry parameters.

BRIEF DESCRIPTION OF PROGRAMS USED IN THIS STUDY

Reference 1 describes linearized theory methodology and an associated computer program for the design of wing lifting surfaces with attainable thrust taken into consideration. The approach is based on the determination of an optimum combination of a series of candidate surfaces rather than the more commonly used candidate loadings. Special leading-edge surfaces are selected to provide distributed leading-edge thrust forces which compensate for any failure to achieve the full theoretical leading-edge thrust, and a second series of general candidate surfaces are selected to minimize drag

subject to constraints on the lift coefficient and, if desired, on the pitching moment coefficient. A primary purpose of this design approach is the introduction of attainable leading-edge thrust considerations so that relatively mild camber surfaces may be employed in the development of aerodynamic efficiencies comparable to those attainable if full theoretical leading-edge thrust could be achieved. The program also is applicable to the design of sharp leading-edge wings, which is actually just a limiting case of the attainable thrust design. A special feature of the program permits the design of mission adaptive surfaces--special leading-edge and trailing-edge surface modifications that may be employed for improved performance at specified flight conditions. The program provides an analysis as well as a design capability and is applicable to both subsonic and supersonic flow.

Reference 6 introduced a wing evaluation program that was later expanded to provide for the evaluation of leading- and trailing-edge flap systems in reference 3 and also provided the subsonic wing surface evaluation capability of the wing design program. The methodology and computer program of reference 6 provide estimates of the subsonic aerodynamic performance of trwisted and cambered wings of arbitrary planform with attainable thrust and vortex lift considerations taken into account. The computational system is based on a linearized theory lifting surface solution which provides a spanwise distribution of theoretical leading-edge thrust in addition to the surface distribution of perturbation velocities. In contrast to the commonly accepted practice of obtaining linearized theory results by simultaneous solution of a large set of equations, this method relies on a solution by iteration.

Reference 3 describes a revised wing evaluation program that provides for the simultaneous analysis of up to 25 pairs of leading-edge and trailing-edge deflection schedules of simple hinged low-speed flap systems in addition to the analysis of twisted and cambered wings of arbitrary planform.

Both the design program (reference 1) and the evaluation program (reference 3) employ constant size elements, except at the wing leading and trailing edge. This arrangement is well suited to the handling of special design areas and leading- and trailing-edge flap regions.

The computer programs:

"WINGDES - Design of Wing Surfaces at Subsonic or Supersonic Speeds" LAR-13315

"SUBAERF - Aerodynamic Analysis of Low-Speed Wing Flap Systems" LAR-13116

may be obtained for a fee from:

Computer Software Management and
Information Center (COSMIC)
112 Barrow Hall
University of Georgia
Athens, GA 30602
(404) 542-3265

DESIGN OF CANDIDATE FLAP SYSTEM

The wing design program, "WINGDES," described in reference 1 will first be applied to the design of flap systems for a thin wing with a sharp leading edge. In another section of this report, design of flap systems with rounded leading edges will be treated. The design program provides two options which may be used in the selection of candidate flap systems. The first selects an optimized camber surface from a set of candidate surfaces which cover the entire wing area. The second provides for the design of an optimized camber surface selected from a set of candidate surfaces which cover only specified leading and trailing edge areas. This option was developed primarily for the design of "mission adaptive surfaces" to provide improved performance at certain flight conditions through leading- and trailing-edge surface shape modifications which leave the major portion of the wing unaffected.

Whole Wing Design

Application of the wing design program option which covers the entire wing to the selection of a candidate flap system is illustrated in figure 1. The wing planform including the areas allocated to leading and trailing edge flaps is shown in the inset sketch. It is assumed that the leading edge flap system may employ four segments and the trailing edge system may employ two segments. For the sake of simplicity, all of the wing exclusive of the flap areas is assumed to be uncambered and untwisted. The design conditions for this example are a Mach number of 0.5 and a lift coefficient of 0.7. No restraints on pitching moment are applied.

Surface ordinates nondimensionalized with respect to the wing root chord are shown as a function of distance behind the leading edge also nondimensionalized with respect to the wing root chord. Airfoil section mean camber surfaces are shown for five semispan locations from $\frac{y}{b/2} = 0.1$ to $\frac{y}{b/2} = 0.9$. For convenience, the program generated wing camber surface is shown for a reference angle of attack of 0°. Notice, that in addition to the section camber, there is a considerable spanwise twist. This is due to the spanwise growth in upwash at the leading edge for this swept leading edge wing. The wing design process utilizes this upwash to generate lift on surfaces which are inclined so as to produce a distributed thrust force. According to program estimates, this camber surface should provide a relatively high aerodynamic efficiency, a suction parameter of 0.93 at the design conditions. A well-designed flap system should attempt to match as closely as possible the surface and loadings of the camber surface design, with particular attention being given to the wing outboard stations were most of the distributed thrust is developed. The dashed line represents an attempt to approximate the design camber surface through a schedule of deflections of the

leading and trailing edge flap segments as shown in the sketches included in the figure. Note that in order to approximate the outboard section ordinates it was necessary to rotate the flat wing surface to a reference angle of attack of -12.0°. This causes a substantial discrepancy between the two surfaces for the aft portion of the inboard stations. Clearly, a large chord inboard trailing-edge flap would be desirable. In the absence of such a flap, the restricted area trailing edge flap will require large deflections to produce comparable loadings. There is seen to be much more "guess work" involved in selection of trailing-edge flap deflections than in selection of leading-edge flap deflections. Also notice that a larger chord leading-edge flap for the outer segments would provide a better match with the wing design program surface. However, within the constraints of the present problem, the flap deflection schedule represented by the dashed line should provide a reasonably high level of aerodynamic efficiency—less than that of the camber surface, but considerably better than that of the flat wing.

Mission Adaptive Wing Design

In view of some of the uncertainties involved in the use of the whole wing design approach just discussed, the alternate program option for the design of mission adaptive surfaces could be expected to provide an ideal solution. However, the program user needs to be aware of complications that are pointed out in the following example. The same design conditions as used in the whole wing design are applied to the mission adaptive design shown in figure 2. The inset sketch delineates with hatching the wing areas to be affected by the mission adaptive design. Design area chords are taken to be about one and one-half times the actual flap chords. As illustrated in figure 2, this provides a convenient way of defining flap surface slopes by extending the mid region surface to the flap hinge line location and connecting this

point to either the wing leading or trailing edge as appropriate. In using the program for this purpose, it is not necessary or desirable to use a number of trailing-edge candidate surfaces greater than the number of trailing-edge flap segments. For example, a single segment trailing-edge flap would require only the first trailing-edge candidate surface which results in a constant deflection angle. In the present case of a two segment trailing-edge flap, the first two trailing-edge candidate surfaces would define a deflection schedule with a constant term and a linear variation with spanwise position.

Recall that for this design problem no restraint has been placed on pitching moment. Application of the mission adaptive design option to problems of this sort has shown that the numerical solutions tend to call for greater use of leading-edge surfaces and less use of trailing-edge surfaces than would a true optimum design. The difficulty seems to be associated with a design process that uses normal and axial forces instead of lift and drag in the optimization procedures. This is a characteristic common to all linearized theory design methods because a fundamental assumption is that all surface slopes are small. The problem does not arise to any appreciable extent for the whole wing design, but does affect results for the mission adaptive design where relatively large surface slopes are needed to generate the required loadings on restricted areas. An improved design can be found by running the mission adaptive design program for a selected series of design pitching moment coefficients and using a plot such as that shown in the inset sketch of figure 2 to find an improved design. The unrestrained design provides a suction parameter of about 0.89 and a $C_{m,des}$ of about -0.12, whereas an optimum S_S of about 0.92 is seen to occur for a $C_{m,des}$ of about -0.22. This large negative moment might present a trim drag problem in an airplane design project. When horizontal tail or canard trim contributions are

considered in the definition of a desired wing moment coefficient and that moment is specified as a wing design program input, a better overall design should result. In that case, the previously described search for optimum performance of the wing alone is avoided.

The solid line shown on the ordinate plot of figure 2 shows the selected design corresponding to a $C_{m,des}$ = -.22 restraint. This mission adaptive design clearly simplifies the task of defining flap deflection schedules that approximate the camber surface. The deflection schedules called for are not greatly different than those that resulted from the whole wing design. The primary difference is in the trailing edge schedule which probably is the result of the imposition of the moment restraint. The selected mission adaptive camber surface design has a suction parameter only slightly less than that of the whole wing design. Subsequent evaluation of the performance potential of the two candidate flap systems showed only negligable differences. Therefore, the detailed analysis of the estimated flap system performance to be covered in the following section of this paper will be for only one of the systems, that generated by the whole wing design.

THEORETICAL EVALUATION OF CANDIDATE FLAP SYSTEM

The aerodynamic performance of the candidate flap system can not be expected to match that of the cambered and twisted wing surface from which it is derived. First, the flap-mean camber surface is only an approximation of the designed surface, and the connected straight line airfoil is inherently less efficient than the continuous curve. Second, the sharp leading edge and the surface breaks at the hinge lines of the flaps can induce flow separation which may lead to further performance decrements. The flap system evaluation of reference 3 can account for the first of these effects and thus can provide an estimate of the aerodynamic performance potential associated with a

predominantly attached flow. It should be noted, however, that for this program an accurate numerical analysis requires deflected flap surfaces to be represented by no less than two program elements for the smallest flap chord. Reference 1 gives a simple way of estimating, on an average basis, the number of elements that can be expected to be included in a given chord.

Performance of Candidate Flap System

Predictions of the aerodynamic performance of the candidate flap system, with the nominal flap deflection schedules depicted in figure 1, given by the wing evaluation program, "SUBAERF", are shown in figure 3. The lift-drag polar curve of the wing with flaps is compared with that of the cambered wing from which the flap system was derived and with that of the flat wing (undeflected flaps). These program results are also compared with theoretical limits for a wing with an elliptical span load distribution (uniform downwash) and for a flat wing without leading-edge thrust or separated flow vortex forces. At the design lift coefficient, the wing with flaps is estimated to be capable of producing at best a suction parameter of about 0.77 compared to the cambered wing suction parameter of about 0.93.

Performance of Flap System Family

In addition to the data for the nominal flap deflection schedule shown in figure 3, the wing analysis program can also provide similar data for smaller and larger deflections of either leading- or trailing-edge flaps. The tangents of the nominal set of deflection angles are multiplied by program input factors. Up to 5 leading-edge multiplication factors (including the nominal value of 1.0) and up to 5 trailing-edge multiplication factors (including the nominal value of 1.0) may be employed. The program provides data for all possible combinations up to the maximum of 25. This capability makes it possible to collect, with little additional effort, the data

necessary for the preparation of performance maps such as that shown in figure 4. The map contour lines show combinations of leading-edge and trailing-edge factors that produce a given performance level as defined by the suction parameter.

It is seen that the peak performance, a suction parameter of about 0.77, is achieved for leading-edge and trailing-edge factors that are both close to 1.0. In view of the uncertainty in the selection of trailing-edge flap deflection angles, such a close correspondence cannot normally be expected. If the optimum performance had been found to occur for deflections far different than the nominal values it would have been necessary to redefine the nominal values because the program results are most accurate for deflections at the nominal values. Aerodynamic characterics for other deflections are found by use of perturbation methods which introduce some inaccuracies.

Notice that there is a wide range of deflection combinations that yield performance levels not much lower than that of the optimum combination. There is seen to be an inverse relationship between leading-edge and trailing-edge deflections. An increase in trailing-edge deflection requires a decrease in leading-edge deflection to retain good performance levels. As will be seen later, when the possibility of excessive flow separation is suspected there is an advantage to be gained by favoring larger trailing-edge deflections and smaller leading-edge deflections. In explaining the relatively good performance attainable with the trailing-edge flaps alone it may be helpful to think of the remainder of the wing as a very large area leading-edge flap.

Comparison of Wing with Flaps and Cambered Wing

Figure 5 will help to illustrate the way in which the wing with the candidate flap system (with the nominal flap deflection schedule of figure 1) approaches the surface shape and pressure loadings of the cambered wing. At

the left of the figure, nondimensionalized surface ordinates are shown as a function of nondimensionalized distance behind the leading edge for 5 representative semispan stations. These ordinates represent the wing at the attitude required for generation of the design lift coefficient of 0.7. At the right of the figure are shown the lifting pressure distributions for the same semispan stations at the lift coefficient of 0.7. Note particularly the outboard stations where a considerable portion of the loading is developed on the front of airfoil section where the surface slopes will provide a thrust rather than a drag force. This is made possible by the upwash field ahead of the wing leading edge which is generated in large part by the forward and inboard regions of the wing. The flap system was selected to approach as closely as possible (within the design restraints) the surfaces and loadings of the optimized cambered wing. As can be seen in this figure and in the previous data, a reasonable selection has been made. A difficulty that may be anticipated in the actual performance of the flap system is associated with the pressure peaks that occur at the leading edge and at the hinge lines. Except at very high Reynolds numbers, it may not be possible to reach pressure levels which satisfy the requirements for attached flow around sharp corners. As will be explained later, the most severe impact on performance may be due to the separation that can occur at the leading-edge flap hinge line.

Effect of Leading-Edge Flap Deflection

The sensitivity of the flap system performance to leading-edge flap deflection may be explored with the aid of figure 6. Section normal and axial force coefficients are shown as a function of leading-edge flap deflection angle for each of four semispan stations at or near the flap segment midpoint. The vertical dashed line shows the nominal candidate flap system

deflection angle for each segment as shown on the schedule plots of figure 1. As pointed out before, these angles produced the best performance for the flap system family and thus are also the optimum angles. For these plots, as the deflection angle of a given segment is altered, the deflection angles of the other segments are not held constant at the nominal angles but are increased or decreased in unison by the same proportions relative to the nominal values. The trailing-edge flap angles are held constant at the nominal values indicated on the inset sketch. As leading-edge flap deflections are increased in unison, the wing angle of attack is increased to preserve the design lift coefficient of 0.7.

For the outer three wing semispan stations the section normal force coefficient decreases with increasing leading-edge flap deflection angles. For the inboard station, however, the increasing wing angle of attack more than compensates for the loss of the flap loading, and the section normal force increases with increasing deflection. The generally higher level of section axial force coefficient for the two inboard semispan stations is due primarily to the larger trailing-edge flap deflection (20° for the two inboard stations, 10° for the two outboard). The section axial force first decreases with increasing deflection angle, reaches a minimum, and then increases with further deflection. As the leading-edge deflection angle increases the frontal area projection on which thrust can be realized increases as the sine of the angle. At the same time, the loading to produce such a thrust decreases uniformly until at some point the loading goes to zero. Well before that occurs, a point of diminishing returns is reached where the thrust contribution is maximized. The optimum aerodynamic performance of the flap is reached somewhat before the axial force minimum because of the decreasing normal force. Note the general tendency to a requirement for larger

deflection angles with increasing semispan station. The optimum deflection is dependent on the local upwash which increases with increasing semispan station until it reaches a maximum somewhat inboard of the wing tip.

The Role of the Vortex Force

As stated at the outset of this study, it is presumed that maximization of flap system aerodynamic performance requires flow patterns that insofar as possible are predominantly attached. However, for the sharp leading-edge flaps now being discussed, completely attached flow is not possible; thus it would be of interest to examine the contribution made by the separated leading-edge vortex forces. For this purpose, the accounting system of the Polhamus leading edge suction analogy (reference 4) is employed. For a flat wing section with a flow that separates at the leading edge and reattaches before the trailing edge, the vortex force is set equal to the leading edge suction force $(c_t/\cos\Lambda)$. In other words the leading edge thrust is not lost when the flow separates, but appears as a normal rather than an axial force. The normal force associated with the potential flow about the section in the absence of separation is undiminished. The vortex force is thus simply an additional normal force component yielding a nonlinear variation of normal force and lift with angle of attack. That system is retained in the present program analysis, except that the theoretical leading-edge thrust coefficient accounts for a wing camber surface or a deflected flap surface according to the method described in reference 6, and an estimate of the vortex force distribution is provided as described in reference 2.

Figure 7 shows the contribution of the vortex force to section axial force at an outboard wing semispan station ($\frac{y}{b/2} = 0.7$) for the two vortex location options provided by the wing evaluation program of reference 2. The plots show axial force coefficient as a function of leading-edge flap deflec-

tion angle, and the inset sketches show section profiles and program pressure distributions for selected deflection angles. At the left of the figure data are shown for a vortex location option based on experimental data for flat sharp leading edge delta wings. Here, the program calculated vortex contribution to axial force is negligible because, even for angles near the optimum, the vortex is distributed over much of the section chord, and there is only a small loading on the deflected flap where a thrust can be generated. The vortex location option developed by Lan in reference 7 places the vortex much closer to the wing leading edge. As shown at the right of the figure, this option indicates a much more substantial contribution of the vortex force to the section axial force. With this option, the program gives an improved wing overall suction parameter of about 0.83 (compared to about 0.77 for the other option) which occurs for smaller deflection angles. Even with this option, however, the vortex contribution is only about 15 percent of the total force on the leading edge flap. There is only a small amount of data currently available to show which of these two location methods provides the more accurate estimates for deflected leading edge flaps. The matter can also be further complicated by the choice of numerical methods for the calculation of theoretical leading-edge thrust.

For reasons to be discussed later, it may be desirable to have the flow which separated at the leading edge return to the surface at the leading-edge flap hinge line. This design principal for "vortex flaps" has been suggested in reference 5. For the delta wing vortex location option, this condition is not reached until the leading-edge flap deflection angle reaches 40°. Thus if flow reattachment at the hinge line is essential to good real flow performance and the delta wing vortex location option is correct, there would be a small performance penalty relative to the theoretical potential flow optimum

solution. For the vortex location option given by Lan, reattachment at the hinge line occurs at a deflection angle of less than 10° and there would be a substantial performance penalty relative to the performance estimates given by the wing evaluation program. If, as is likely, the correct vortex location is somewhere between those given by the two options; there is a good possibility that the hinge line reattachment condition would correspond to relatively good theoretical performance levels.

COMPARISON OF THEORETICAL AND SEPARATED FLOW

The preceding discussion, which indicates that forces associated with flow separation are a small part of the total, seems to support the contention that the flow about properly designed flap systems may be predominantly attached, even for wings with sharp leading edges. The relationship between attached flow and separated flow for flap systems may be further explored with the aid of the sketches of figure 8. This figure depicts schematically the theoretical attached flow and the postulated separated flow about a sharp leading-edge wing section with three different leading-edge flap deflections. Sketches also show the corresponding chordwise pressure distributions.

At the left of the figure are shown sketches for a small leading-edge flap deflection. For the theoretical attached flow the mean camber surface with its sharp breaks in direction leads to a pressure distribution with sharp peaks (actually singularities for a true analytic solution). With a sharp leading edge the actual flow would detach at the leading edge and form a separated boundary layer flow region. For the purposes of the following discussion the postulated flow is assumed to reattach ahead of the trailing edge flap hinge line. The general character of the flow field for either attached or separated flow is determined by streamlines just outside of the edge of the boundary layer which are depicted here by the arrows. Just the

presence of the boundary layer, separated or not, will tend to soften the pressure peaks wherever they occur. For the separated flow, a gradual and general curvature of the flow from the leading edge back to the reattachment point will occur. The lifting pressure distribution induced by the potential flow outside of the boundary layer could be approximated by use of lifting surface theory applied to an effective mean camber surface such as that shown in the sketch. For the purposes of this analysis, however, that step is not necessary. It is sufficient to note that the resultant lifting force over a given chordwise distance may be equated to the net change in downward momentum of the flow. Thus, if the upwash just ahead of the leading edge is the same for both flow situations, and the separated flow reattaches before the trailing edge, the total potential flow lifting force will be the same for both attached and separated flow. Within the separated flow region, there will be circulation patterns generated by the shed vorticity of the leading edge associated with the loss of leading edge thrust. This will contribute to the overall lifting force to create a somewhat greater total for separated flow. But, of course, the distribution for the separated flow would be different, and, for the situation shown here, separation could lead to a loss in aerodynamic efficiency. This could happen because delay of the major part of the flow turning to further aft positions would result in a loss of the distributed thrust on the deflected flap surface.

At the center of the figure, flow patterns and pressure distributions for a moderate leading-edge deflection are shown. With the leading edge more nearly aligned with the upwash ahead of the wing, a reduced vortex force and a smaller separated flow region would be expected. For the purposes of this discussion, the flow is assumed to reattach at the leading-edge flap hinge line. The net change in downward momentum from just ahead of the wing leading

edge to a point just aft of the leading-edge flap hinge line will be the same for both attached and separated flow, and the potential flow force on the flap itself will also be the same for both flow patterns. With the small vortex force associated with circulation within the separated region taken into account, the total loading on the flap will be somewhat larger for separated flow than for attached. Thus there will be no loss in lifting efficiency for the separated flow relative to the attached flow except for the exchange of the theoretical thrust for the less efficient vortex force. But since the sharp leading edge precludes the attainment of any leading-edge thrust, the degree of flow separation considered here is actually an advantage. The flow depicted here would be considered to be predominantly attached. If the flow reattaches ahead of the hinge line, it may not be able to negotiate the sharp turn at the hinge line without separating there. This could lead to a loss in lifting efficiency because some of the flow turning that otherwise would occur at the deflected flap would be felt further aft and would result in a loss of thrust. Reattachment aft of the hinge line also would lead to losses in efficiency for reasons previously discussed.

The data of figure 7 showed that good theoretical performance can extend to leading-edge flap deflections that are large enough to essentially place the leading edge in alignment with the upwash field and reduce the loading just behind the leading edge to nearly zero. Good performance for such large deflections depends on a concentration of lifting pressure at the hinge line. As shown by the sketches at the right of figure 8, a flow separation initiated at the hinge line of a highly deflected leading-edge flap could lead to severe performance penalties. With the leading edge essentially aligned with the flow ahead, all of the turning (which for a flat wing occurs at the leading edge) must now be delayed to the hinge line. Pressure peaks of

similar magnitude and having similar tendencies for the flow to separate may be expected. As shown in the sketches, the delay of the upper surface turning to a location further aft can result in a drastic loss in the beneficial loading on the leading-edge flap surface itself. This obviously is a situation in which the flow cannot be considered to be predominantly attached. A possible solution to the hinge line separation problem could be a design that would provide a smoothing of the sharp corner to allow gradual turning of the flow rather than sharp a change in direction at the hinge line itself.

In the preceding discussion, leading-edge flap loadings were seen to be sensitive to the degree of flow separation. A simple analysis based on the sketches of figure 9 serves to indicate the sensitivity of flap system aerodynamic performance (lift and drag characteristics) to changes in flap loading.

For leading-edge flaps, as shown at the left of the figure, a change in loading on the flap surface itself will produce changes in lift and drag coefficients given by the equation:

$$\frac{dC_D}{dC_L} = \tan(\alpha - \delta_L).$$

The negative sign applied to the flap deflection angle means that in most cases, a decrease in lift caused by a loss in the leading-edge flap loading will be accompanied by an increase in drag. As for the sample case shown here, there will be a tendency at the design point for the lift and drag changes to follow a line more nearly perpendicular to than tangent to the lift-drag curve. Flap system aerodynamic performance will therefore be extremely sensitive to the leading-edge flap flow conditions (the degree of separation).

For the trailing-edge flap shown at the right of the figure, the situation is quite different. Changes in lift and drag given by the equation:

$$\frac{dC_D}{dC_L} = \tan(\alpha + \delta_T)$$

mean that a loss in trailing-edge flap loading is likely to introduce only small changes in lift to drag ratio in the vicinity of the design point. There is even an indication that if trailing-edge flap deflections are unnecessarily high, flow separation could compensate and bring about a drag reduction. In any case, flap system aerodynamic performance will be much more sensitive to flow separation affecting the leading-edge flaps than to flow separation affecting the trailing-edge flaps.

DESIGN WITHOUT FLAP SEGMENTATION

If leading-edge flap segmentation is not permitted, the flap design problem is less ammenable to the procedures previously outlined. For a straight hinge line and constant leading-edge flap deflection, it may not be possible to define flap surfaces that reasonably approximate the wing design camber surface. One way of handling this problem is to use the program of reference 3 to evaluate a limited series of candidate flaps and from this data select an optimum for that series. For the wing of the example just treated, it is clear from the design data that the flap chord at the wing tip should be as large as the design limitations allow. The remaining problem is the selection of the hinge-line sweep angle. This can be accomplished by a series of three or more wing evaluation program runs with different hinge-line sweep angles which are used to define the variation of the suction parameter with sweep angle and to select an optimum angle. For the design problem treated here, such a process indicates that the hinge-line should be at the rear limit

of the available flap area and that optimum flap deflection angles are about 20° for the leading-edge flaps and about 15° for the trailing-edge flaps. These deflections produce a suction parameter of about 0.74 at the $C_L = 0.7$ design condition. As might have been expected, this aerodynamic efficiency is somewhat less than that indicated for the segmented leading-edge flaps. This selection process for the selection of simple unsegmented leading-edge flaps will of course not always result in full use of the available flap area. In many cases, espcially for wings with rounded leading edges which produce leading-edge thrust, reduced inboard flap chords and perhaps inverse taper will be called for.

PROGRAM PREDICTION OF FLAP SYSTEM PERFORMANCE

Up to this point, the use of a wing design program for selection of a candidate flap system has been described, the use of a wing evaluation program for estimation of flap system aerodynamic performance potential has been illustrated, and possible sources of descrepancies between theoretical attached flow and actual separated flow have been explored. It might now be appropriate to illustrate the capability of the evaluation program to provide estimates of experimental results for a representative flap system. (At this time experimental data for flap systems designed according to proceedures outlined herein are not available.)

In an experimental investigation recently conducted in the NASA Langley High-Speed 7- x 10-Foot Wind Tunnel, sufficient data were obtained to permit the construction of a suction parameter contour map similar to that of figure 4. Experimental data from that investigation together with a program analysis are shown in figure 10. The wing planform including the leading- and trailing-edge flaps are shown in an inset sketch. The test data was obtained at a Mach number of 0.5 and a Reynolds number of 2.9×10^6. Although the leading edge was not sharp, the actual leading edge radius was very small.

An examination of the correspondence between the program and experimental contour maps shows a reasonably good agreement of the maximum suction parameters and the deflection angles at which they were obtained. Apparently, the test Reynolds number was sufficiently high for the flow to be predominantly attached for flap deflection combinations near the optimum, so that an attached flow theory could account for the wing behavior. For large leading-edge flap deflections, the experimental suction parameters are considerably poorer than the program predictions. This may be the result of hinge line separation which, as discussed previously, can cause a loss of the upper surface loading on the flap surface itself. There is also a poorer measured performance for the wing with undeflected flaps than is predicted by the program. This may be due at least in part to a failure of the leading-edge separated flow to reattach ahead of the wing trailing edge, particularly on the wing outer panel. A correlation of program and experimental data for low-speed tests of a supersonic transport wing shown in reference 3 indicated a similar ability of the program to provide predictions of flap system performance except for extreme deflection angles. However that data did not provide sufficient coverage of flap deflection angles to allow construction of a performance map.

EFFECT OF LEADING EDGE RADIUS

In the interest of simplicity, the description of the flap system design process has been restricted to wings with sharp leading edges which can develop no leading-edge thrust. Now attention will be given to the influence of attainable leading-edge thrust, made possible through use of a finite leading-edge radius. First, the effect of a change in wing section shape on the performance of sharp leading edge design will be explored. Then the effect on the design process of including leading-edge radius and attainable thrust considerations at the outset will be treated.

Effect on Sharp Leading Edge Design

Figure 11 shows program evaluation data for the candidate flap system nominal flap deflections shown in figure 1 with a rounded leading edge section (NACA 65A004) having replaced the original sharp leading-edge section. There is seen to be a small drag reduction in the region of the design lift coefficient and a larger benefit at off design conditions. This can occur because it is impossible for a flap with a finite number of segments to provide an optimal match of upwash field and flap surface slopes at all points along the leading edge. The leading edge radius provides a small angle range over which full theoretical thrust can be achieved. This, in effect, gives the design a factor of safety. The effect of changes in the leading edge deflection schedule on wing performance is illustrated in the plot of section axial force at the right of the figure. The flap system performance could be improved by a reduction of about 20 percent in leading edge deflection angle across the whole span. This would yield a suction parameter of about 0.81 compared to 0.77 for the sharp leading edge wing flap design. Even when the favorable effect of reattachment of the leading edge separation at the hinge line is considered, the rounded leading edge should still offer an advantage. The rounded leading edge could provide the same reattachment point as does the sharp leading edge but at a smaller deflection angle with leading edge thrust substituted for the less efficient normal force.

Effect on Rounded Leading Edge Design

The wing design computer program of reference 1 can be used to define an optimized wing camber surface with attainable leading edge thrust taken into account. As pointed out in that reference, the inclusion of attainable

leading-edge thrust will tend to yield milder camber surfaces. In fact for a sufficiently thick wing at a high enough Reynolds number, the program design could call for a completely flat camber surface. For the same design problem as treated previously (see figure 1) but with an NACA 65A004 section substituted for the sharp leading edge section, the camber surface shown in figure 12 is obtained. Using the same considerations as in the previous problem, a somewhat different flap system design is obtained. Notice the reduced chords of the two inboard leading-edge flaps. Because an appreciable amount of leading-edge thrust can actually be generated by the inboard sections with their large chord and thickness, there is less need for distributed thrust and reduced chords and reduced deflection angles may be employed. The reduced inboard chords and deflection angles also increase the upwash field on which the performance of the outboard leading-edge flaps depends; or perhaps more correctly allow the upwash to be generated at a smaller wing angle of attack. The leading-edge flap deflections shown in the sketch are consistently smaller than those called for in the sharp leading-edge design. There is no change in the trailing-edge flap deflections.

Evaluation program estimates of aerodynamic performance for the rounded leading edge candidate flap system are given in figure 13. This flap system with the nominal set of deflection angles is estimated to give a design point suction parameter of 0.83 compared to 0.77 for the sharp leading-edge flap design. The milder flap deflections provide even larger off design benefits. Because of the smaller deflection angles, the tendency toward performance-robbing separation at the hinge line should be alleviated. Even so, it would be desirable insofar as possible, to provide a smoothed surface at the flap-wing juncture.

EFFECT OF REYNOLDS NUMBER

A rather detailed examination of the effect of Reynolds number on wing and airfoil section pressure distributions was presented in reference 2. These data showed a consistent tendency toward the achievement of higher lifting pressures (particularly in the leading edge region) with increasing Reynolds number. That reference went on to explore the effect of Reynolds number on the performance of twisted and cambered wings and wings with flaps. Some of the more significant points of that analysis are repeated here.

The special importance of Reynolds number effects on the performance of twisted and cambered wings and wings with leading-edge flaps may be illustrated with the aid of two sketches. In sketch (g) a section of a flat wing with superimposed pressure distributions for two Reynolds numbers is shown. The shaded portion of the pressure loading and the shaded force arrow represent the effect of an increase in Reynolds number. The force arrows at the right represent the resultant pressure force on the section at the lower Reynolds number and the increase in this force due to the increase in Reynolds number. These two forces act in generally the same direction, normal to the wing surface, and thus there is only a small improvement in the lift-drag ratio resulting from the increase in Reynolds number (due to the reduced angle of attack required for a given lift coefficient).
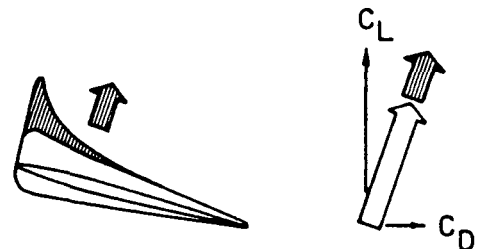
Sketch (g)

For a wing with a leading-edge flap (or a wing with leading-edge camber) the situation can be quite different as illustrated in sketch (h). For such a wing section to perform efficiently the flap must carry a significant load so as to produce a force with a thrust component. This loading will be similar to the loading on the forward portion of a flat wing. As shown by the shaded portion of the pressure distribution and the shaded force arrow, here

Sketch (h)

too, Reynolds number could have a substantial influence on the force generated. But, as shown in the resultant pressure force vectors at the right, the additional force due to the increase in flap loading with Reynolds number, which acts normal to the flap surface, can have a relatively large effect on the resultant drag and the lift drag ratio.

Experimental data showing the effect of Reynolds number on the performance of a twisted and cambered wing are shown in figure 14. The measurements were made at a Mach number of 0.25 and Reynolds numbers of 1.5 and 8.0 million for an aspect ratio 4 delta wing with an NACA 0005-63 wing section. The experimental data is compared with theoretical predictions given by the computer program of reference 3. It will be noted that the higher Reynolds number permits good aerodynamic efficiency to be retained to a substantially higher angle of attack and lift coefficient. The difference is most apparent in the critically important axial force coefficient. The effect of Reynolds number is much more pronounced than the estimate given by the theory which accounts for the change in leading-edge thrust but not the changes in flow separation patterns.

The performance of wings with sharp leading edges is generally believed to be insensitive to changes in Reynolds number. This appears to be true for flat highly swept delta wings, but the generalization may not hold for wings with sharp leading-edge flaps deflected so as to optimize performance. Research data collected for use in the analysis of wind energy systems (reference 8) can be of use in a study of the problem. In that type of research, it is necessary to consider the behavior of airfoils in reversed as well as forward motion. Typical lift curve data for a range of Reynolds numbers are shown in figure 15. The airfoil in reversed flow, of course, has a very sharp leading edge. These data indicate that only above angles of attack of 8° to 10° is the sharp leading-edge airfoil C_L appreciably less sensitive to Reynolds number changes than the rounded leading-edge airfoil C_L. For smaller angles of attack, C_L changes are actually larger for the sharp leading-edge section. Thus, within this Reynolds number range, there will be important Reynolds number sensitivities for sharp leading-edge flaps if the local angle of attack must be restricted to small values to prevent unwanted separation. For the rounded leading-edge airfoil there are likely to be further increases in C_L with increases in Reynolds number above 1.8 million (the lift curve slope for R=1.8 million is still below the potential theory value). For the sharp leading-edge airfoil, increases in C_L with increases in Reynolds number above 1.8 million are likely to occur only for angles above about 6° (up to this point the lift curve for R=1.8 million matches the potential plus vortex lift theory of reference 4). Highly swept flat wings with sharp leading edges apparently are relatively insensitive to Reynolds number changes, even at low Reynolds numbers, because the large growth of upwash along the leading edge causes the outboard wing sections to operate at large effective angles of attack where Reynolds number effects are insignificant. This comparison of

the Reynolds number behavior of sharp and rounded leading-edge airfoils may be affected to some degree by the rounded trailing edge of the airfoil in reversed flow. It would be desirable to also have data for an airfoil with sharp leading edges and sharp trailing edges.

From this discussion, it can be seen that there is a special need for high Reynolds number testing of candidate flap systems. Inadequate Reynolds number test conditions could lead not only to poor prediction of flight performance but also could result in rejection of relatively simple flap systems with excellent high Reynolds number performance but poor low Reynolds number performance. Unfortunately, results from the present study do not provide firm guidelines for acceptable test Reynolds numbers.

CONCLUSIONS

A study of the use of linearized theory computer programs for the design and analysis of low speed flap systems has led to the following conclusions:

(1) From the limited evidence presented herein, it appears that linearized theory numerical methods can represent to a reasonable degree the complex interactions between leading-edge and trailing-edge flaps and can form the basis of a flap design and evaluation system.

(2) Good design practice requires the employment of both leading-edge and trailing-edge flaps.

(3) Near maximum performance can be achieved over a broad range of leading-edge and trailing-edge flap deflection combinations.

(4) Conditions which induce flow separation (thin sections, sharp edges, low Reynolds numbers, and high lift coefficients) may lead to a requirement for leading-edge deflections less than the theoretical optimum and trailing-edge deflections greater than the theoretical optimum.

(5) Practical application of design principles will require careful attention to surface contours (particularly in the vicinity of the leading-edge flap hinge line) to prevent unwanted separation.

(6) Generally, wing sections with a rounded leading edge will provide better performance (with somewhat smaller leading-edge flap deflection angles) than sections with a sharp leading edge.

(7) There can be a very important influence of Reynolds number on flap system performance for both sharp and rounded leading-edge wing sections and there is a special need for high Reynolds number testing of candidate flap systems.

REFERENCES

1. Carlson, Harry W.; and Walkley, Kenneth B.: Numerical Methods and a Computer Program for Subsonic and Supersonic Aerodynamic Design and Analysis of Wings With Attainable Thrust Considerations. NASA CR-3808, 1984.

2. Carlson, Harry W.; Shrout, Barrett L.; and Darden Christine M.: Wing Design with Attainable Thrust Considerations. J.Aircraft, Vol. 22, , No. 3, March 1985, pp. 244-248.

3. Carlson, Harry W.; and Walkley, Kenneth B.: An Aerodynamic Analysis Computer Program and Design Notes for Low Speed Wing Flap Systems. NASA CR-3675, 1983.

4. Polhamus, Edward C.: Predictions of Vortex-Lift Characteristics by a Leading-Edge Suction Analogy. J. Aircraft, Vol. 8, No. 4, April 1971, pp. 193-199.

5. Rao, D. M.: Leading-Edge "Vortex Flaps" for Enhanced Subsonic Aerodynamics of Slender Wings. ICAS-80-13.5, October 1980.

6. Carlson, Harry W.; and Walkley, Kenneth B.: A Computer Program for Wing Subsonic Aerodynamic Performance Estimates Including Attainable Thrust and Vortex Lift Effects. NASA CR-3515, 1982.

7. Lan, C. Edward; and Chang, Jen-Fu: Calculation of Vortex Lift Effect for Cambered Wings by the Suction Analogy. NASA CR-3449, 1981.

8. Jesch, L. F.: and Walton, D.: Reynolds Number Effects of the Aerodynamic Performance of a Vertical Axis Wind Turbine. Third International Symposium on Wind Energy Systems, Lyngby, Copenhagen, Denmark, August 26-29, 1980.
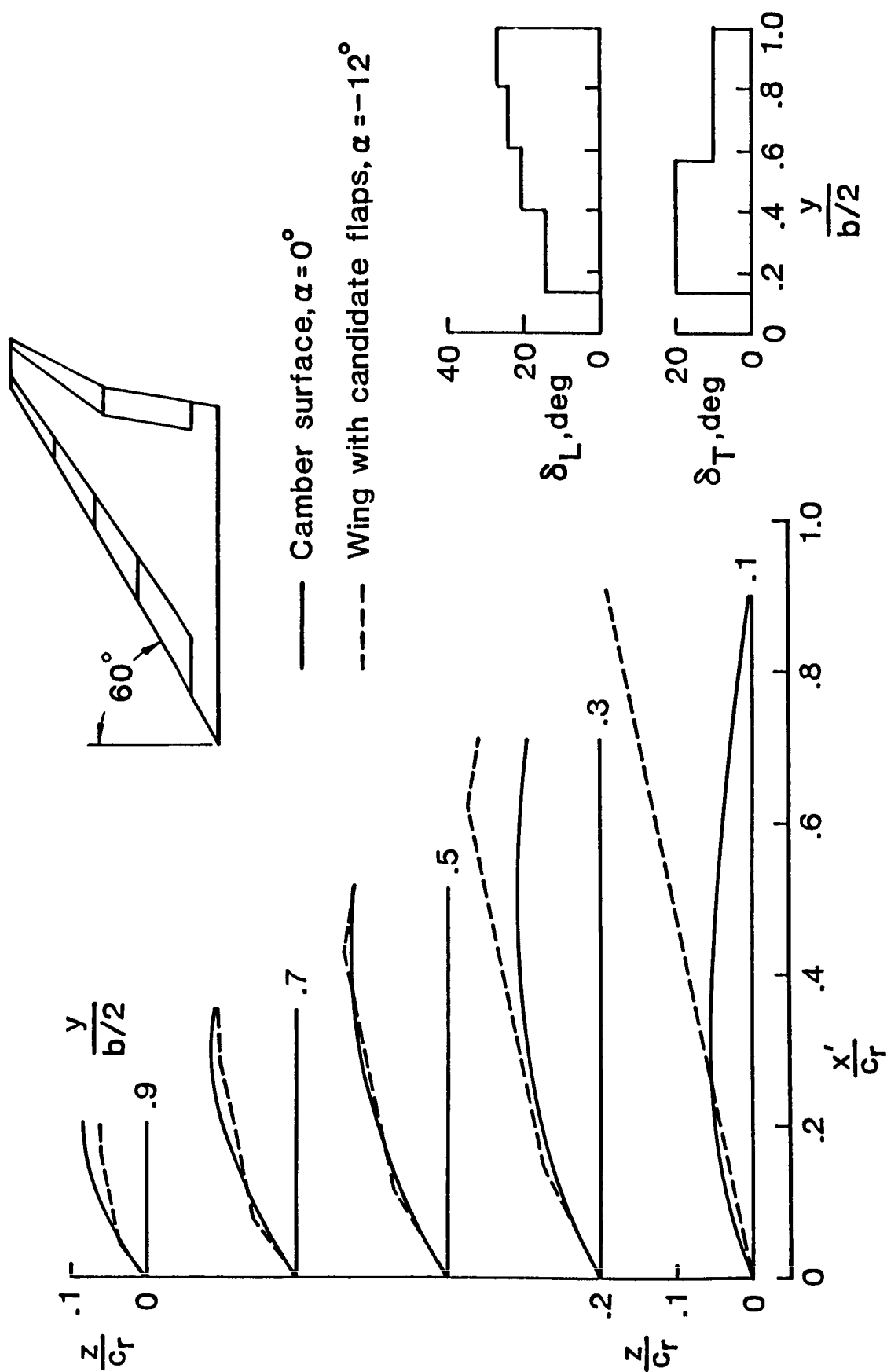
Figure 1. - Use of design program for selection of candidate flap system. Whole wing design for a sharp leading-edge. $M = 0.5$, $C_L = 0.7$.
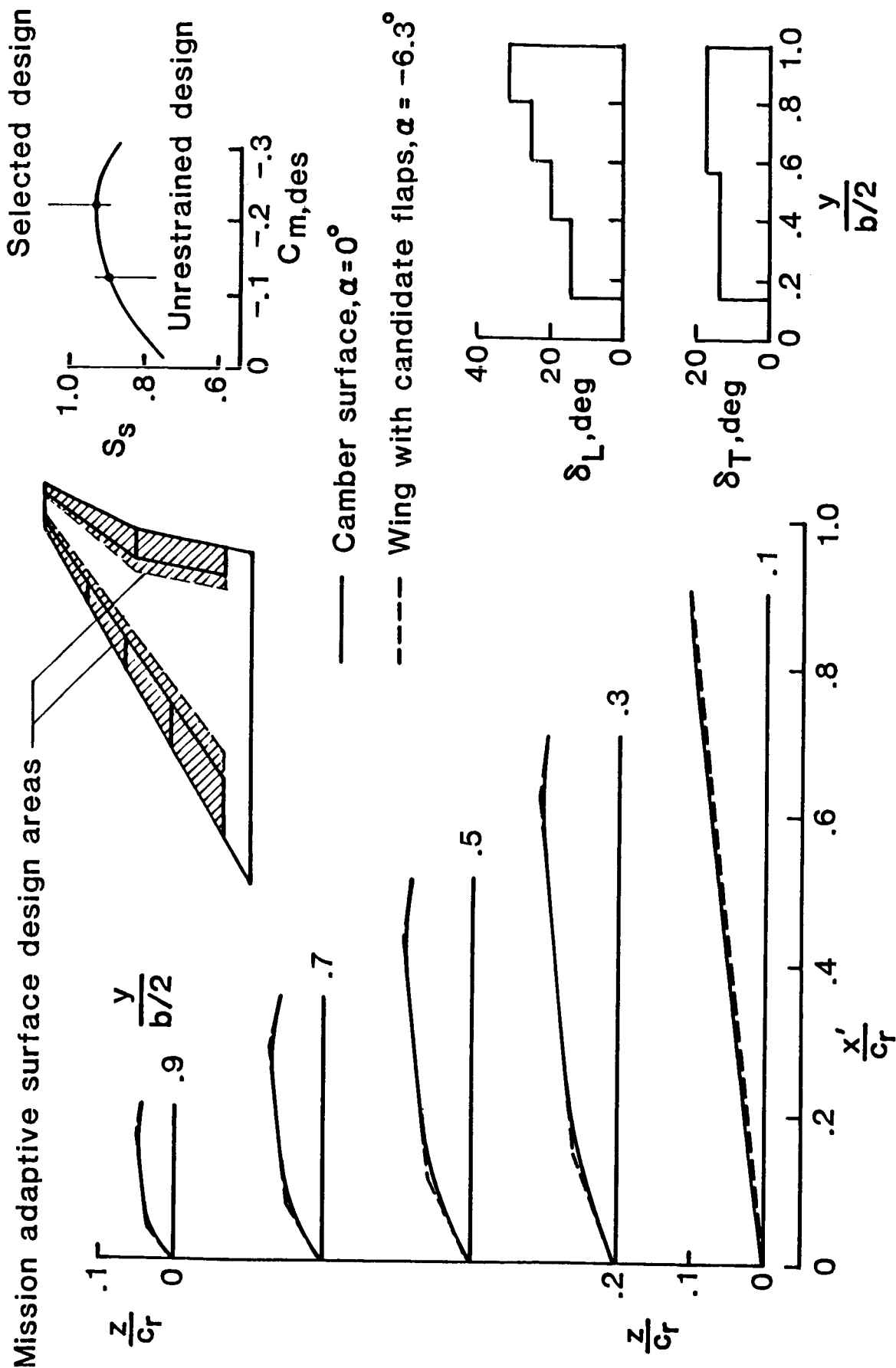
Figure 2. - Alternate use of design program for selection of candidate flap system. Mission adaptive wing design for a sharp leading-edge. $M = 0.5$, $C_L = 0.7$.
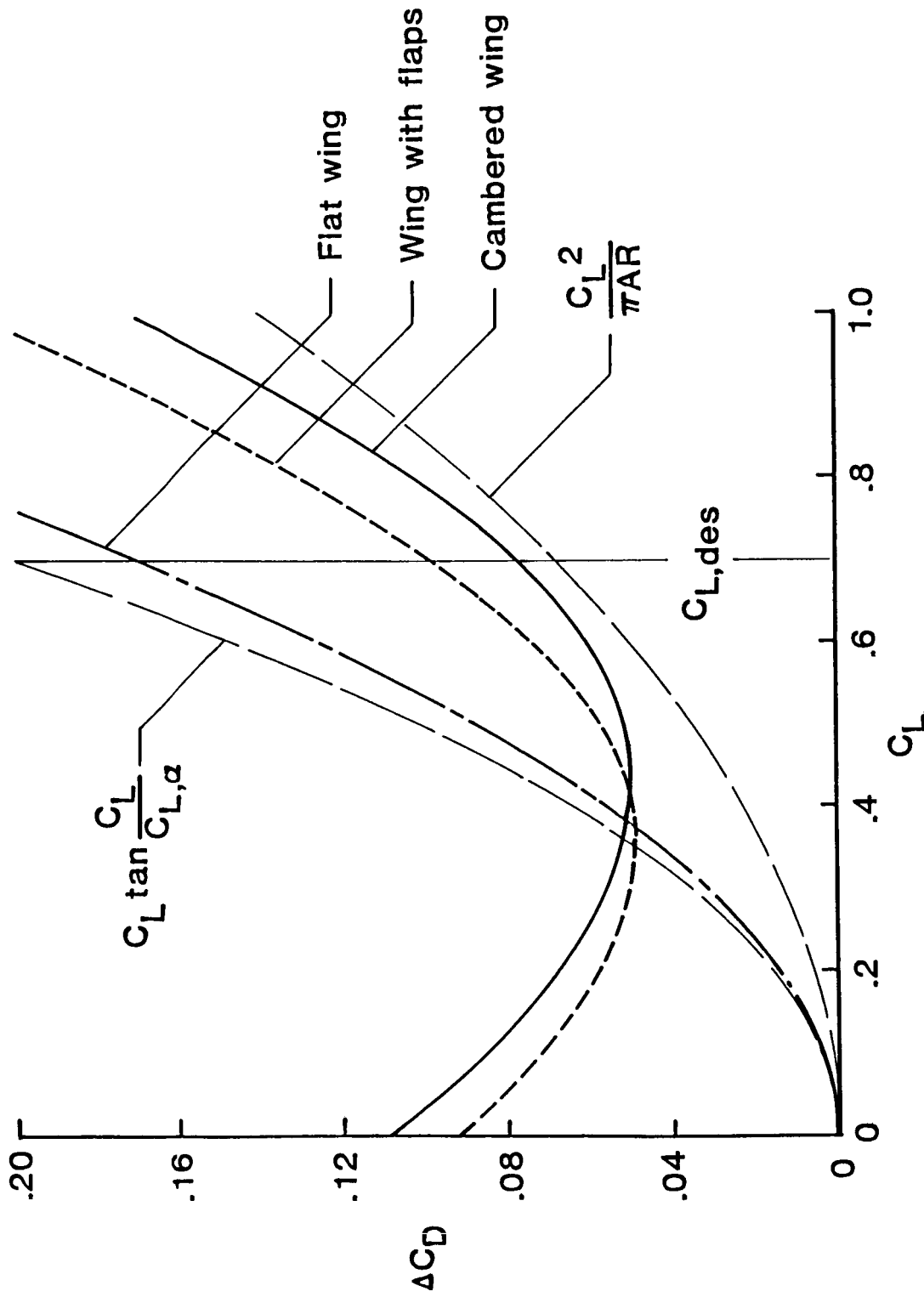
Figure 3. - Lift-drag characteristics of candidate flap system. Sharp leading-edge wing, M = 0.5.
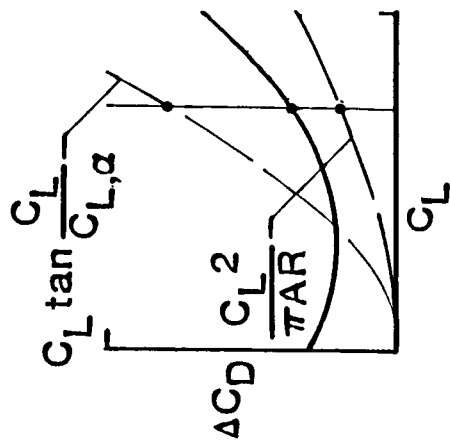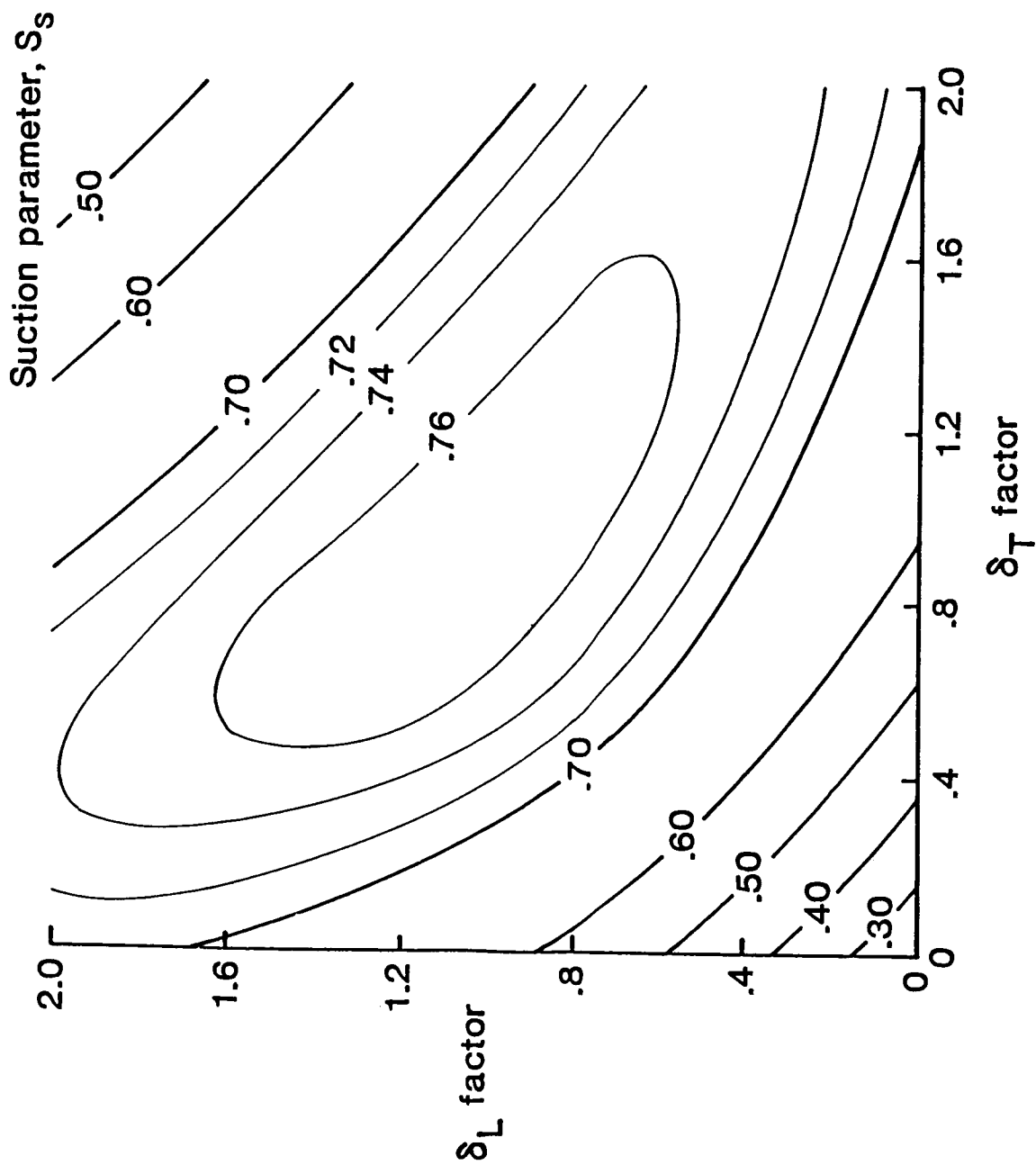
$$S_s = \frac{C_L \tan \dfrac{C_L}{C_{L,\alpha}} - \Delta C_D}{C_L \tan \dfrac{C_L}{C_{L,\alpha}} - \dfrac{C_L{}^2}{\pi AR}}$$

Figure 4. - Performance of candidate flap system family. Sharp leading-edge wing, M = 0.5, C_L = 0.7.
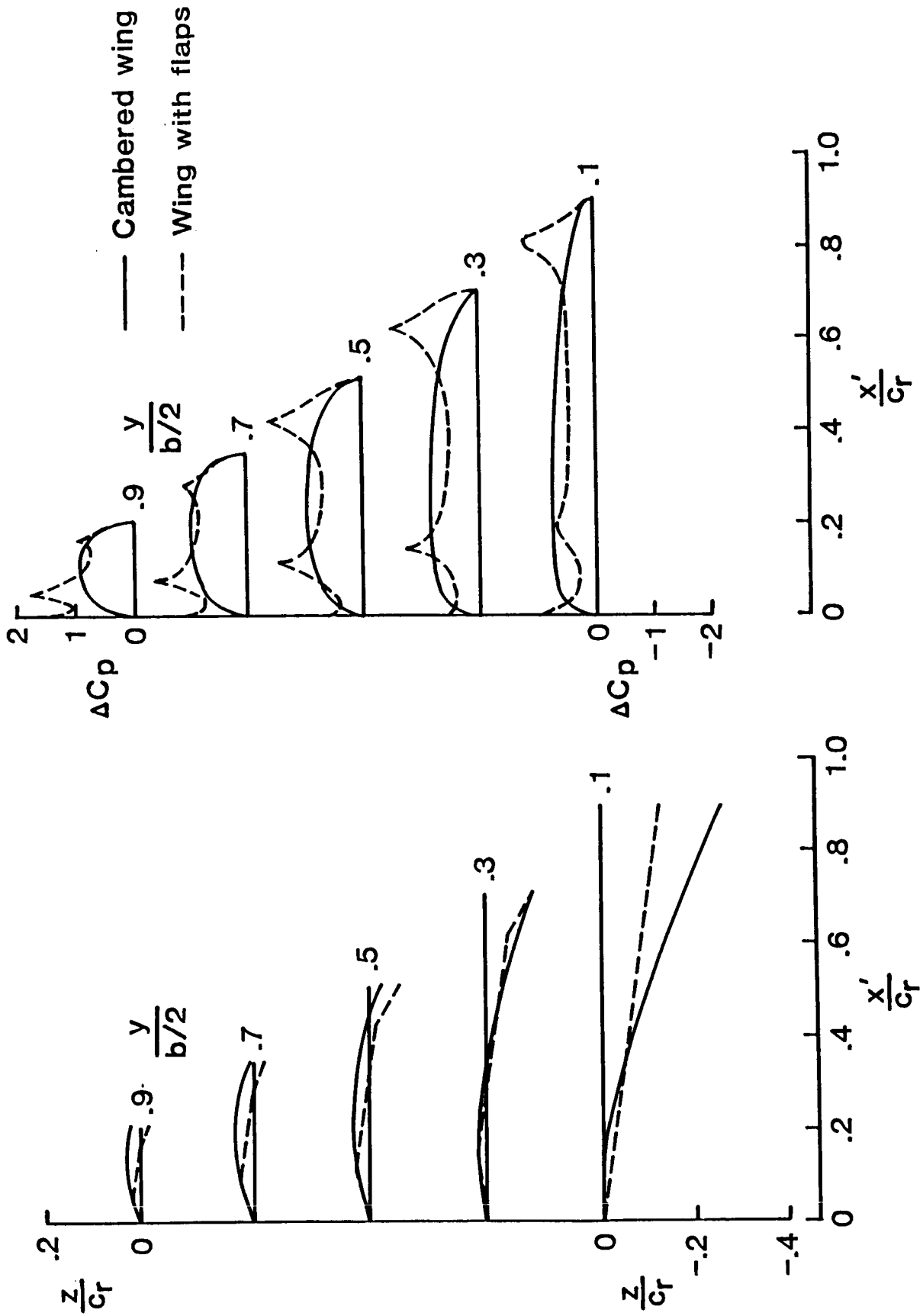
Figure 5. - Comparison of surfaces and loadings of selected flap system with those of the cambered wing. Sharp leading-edge wing, M = 0.5, C_L = 0.7.
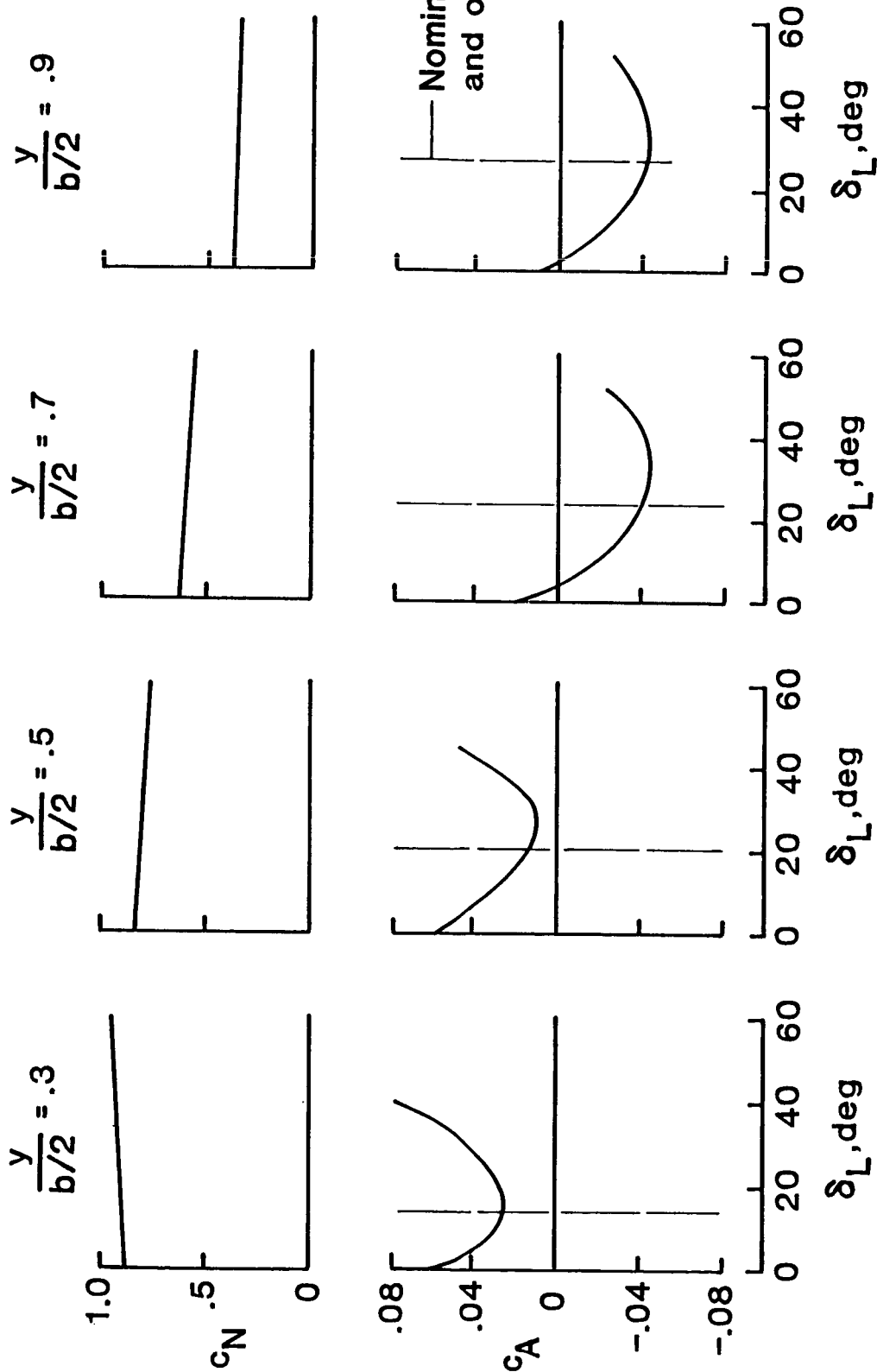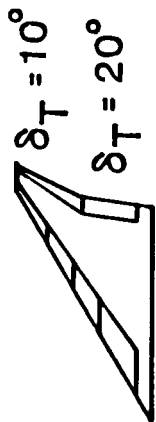
Figure 6. - Effect of leading edge deflection on wing section charac-
teristics. Sharp leading-edge wing, M = 0.5, C_L = 0.7.
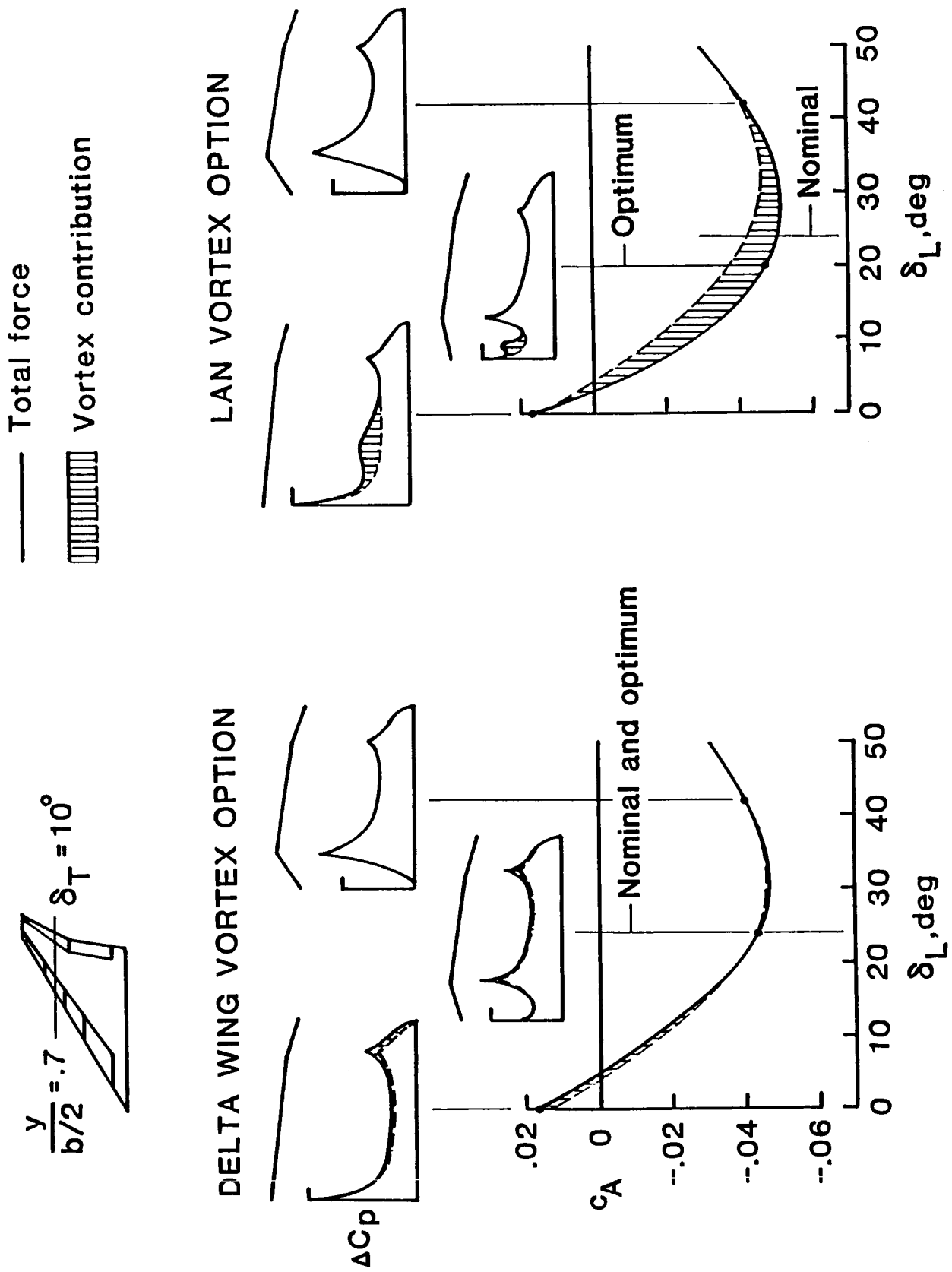
Figure 7. - Contribution of vortex force to wing section characteristics. Sharp leading-edge wing, M = 0.5, C_L = 0.7.
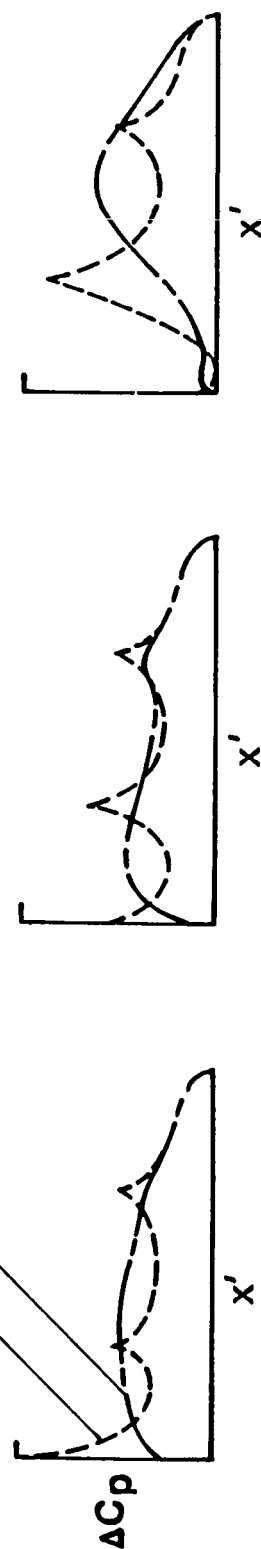
Figure 8. - Comparison of theoretical and separated flow.

LEADING EDGE FLAP

$$\frac{dC_D}{dC_L} = \tan(\alpha - \delta_L)$$
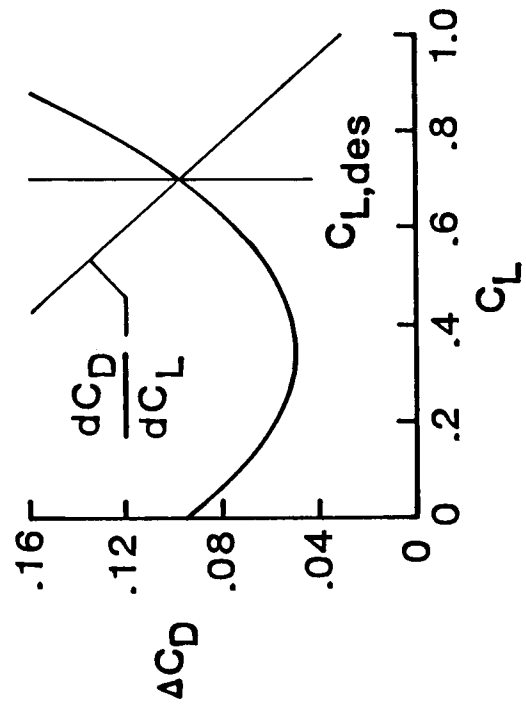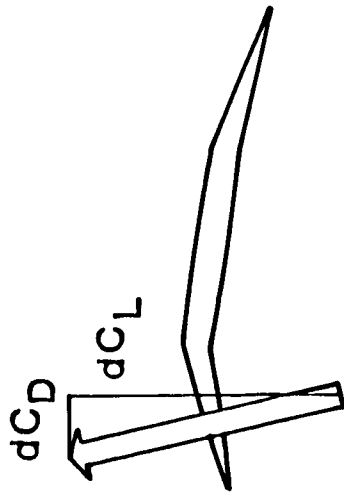
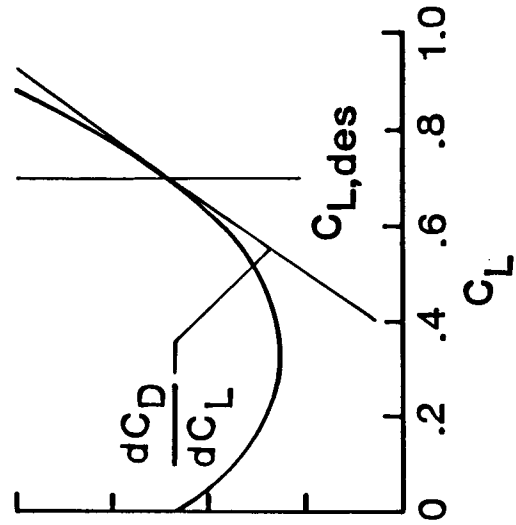TRAILING EDGE FLAP

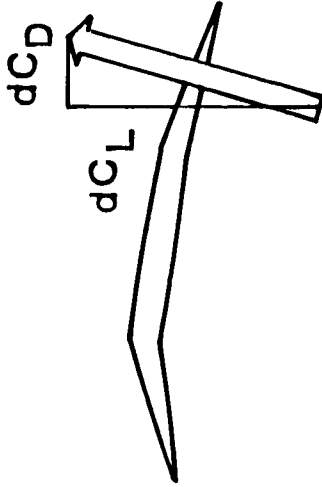$$\frac{dC_D}{dC_L} = \tan(\alpha + \delta_T)$$

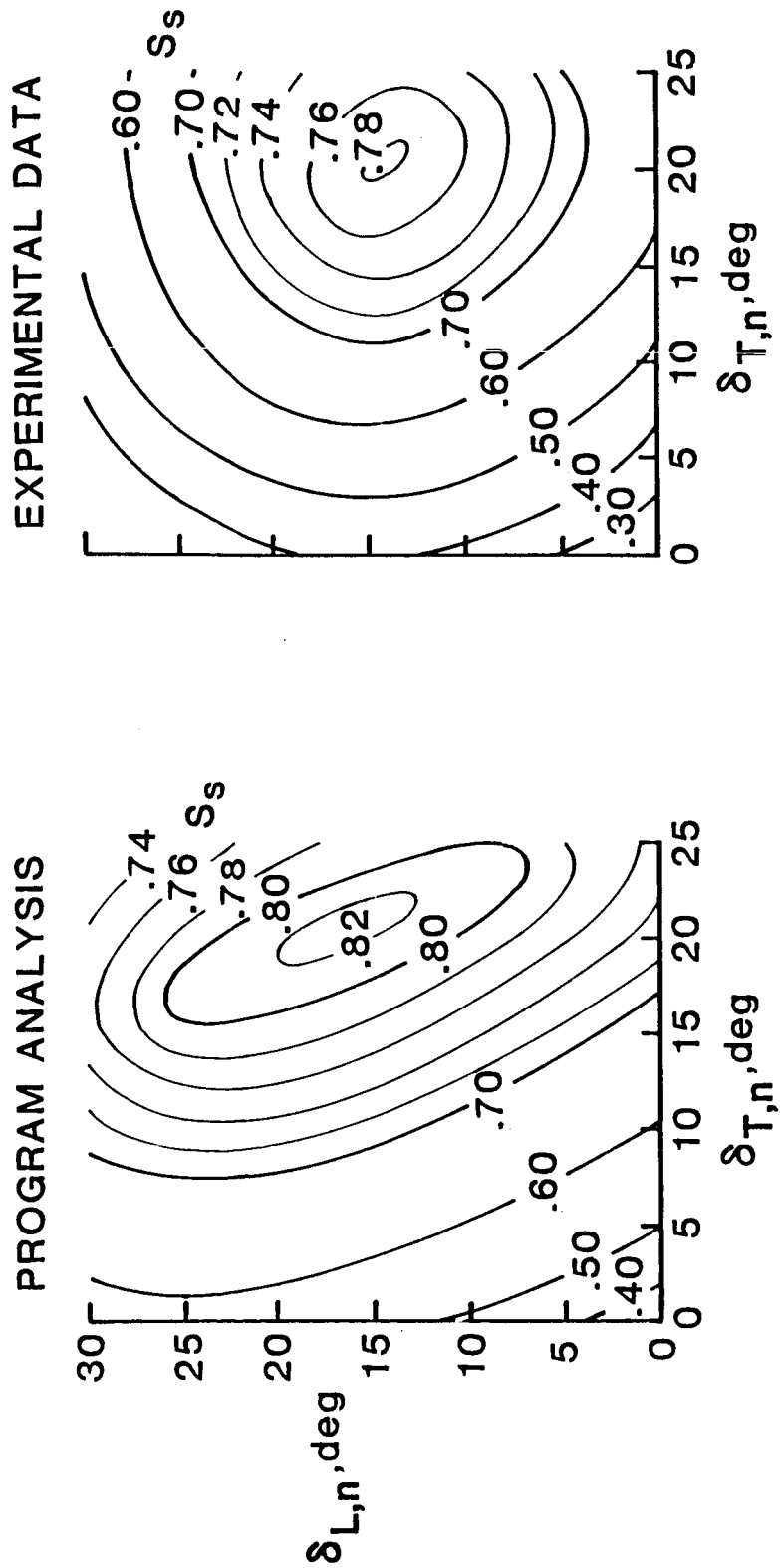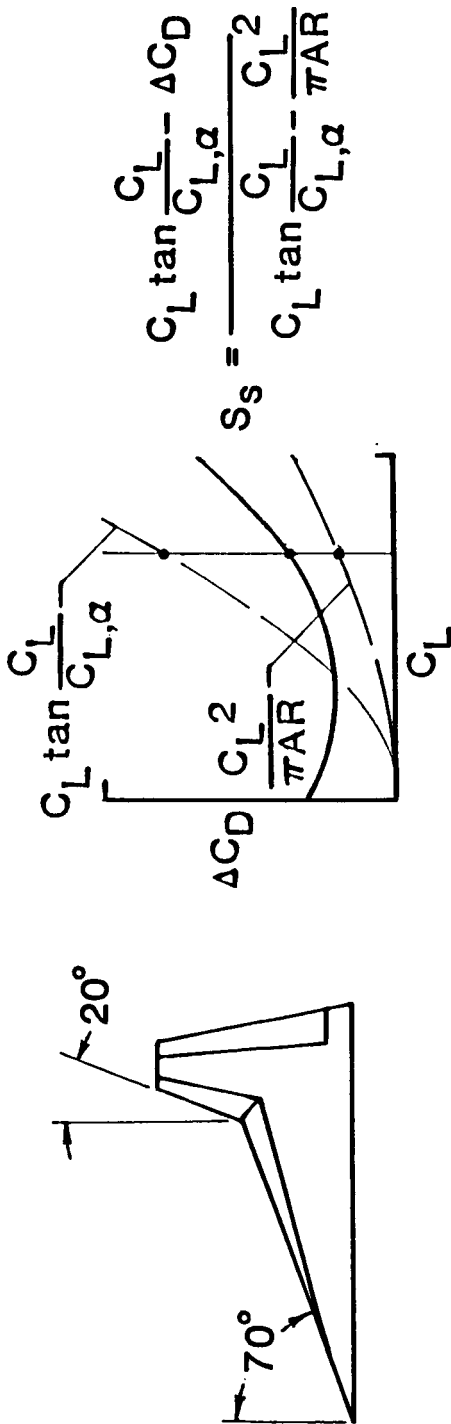Figure 9. - Effect of loading change on flap system performance.

$$S_s = \frac{C_L \tan \dfrac{C_L}{C_{L,\alpha}} - \Delta C_D}{C_L \tan \dfrac{C_L}{C_{L,\alpha}} - \dfrac{C_L^2}{\pi AR}}$$

EXPERIMENTAL DATA

S_s — .60, .70, .72, .74, .76, .78

$\delta_{T,n}$, deg

PROGRAM ANALYSIS

S_s — .74, .76, .78, .80, .82, .80, .70, .60, .50, .40

$\delta_{L,n}$, deg

$\delta_{T,n}$, deg

Figure 10. – Program prediction of flap system performance. M = 0.5,
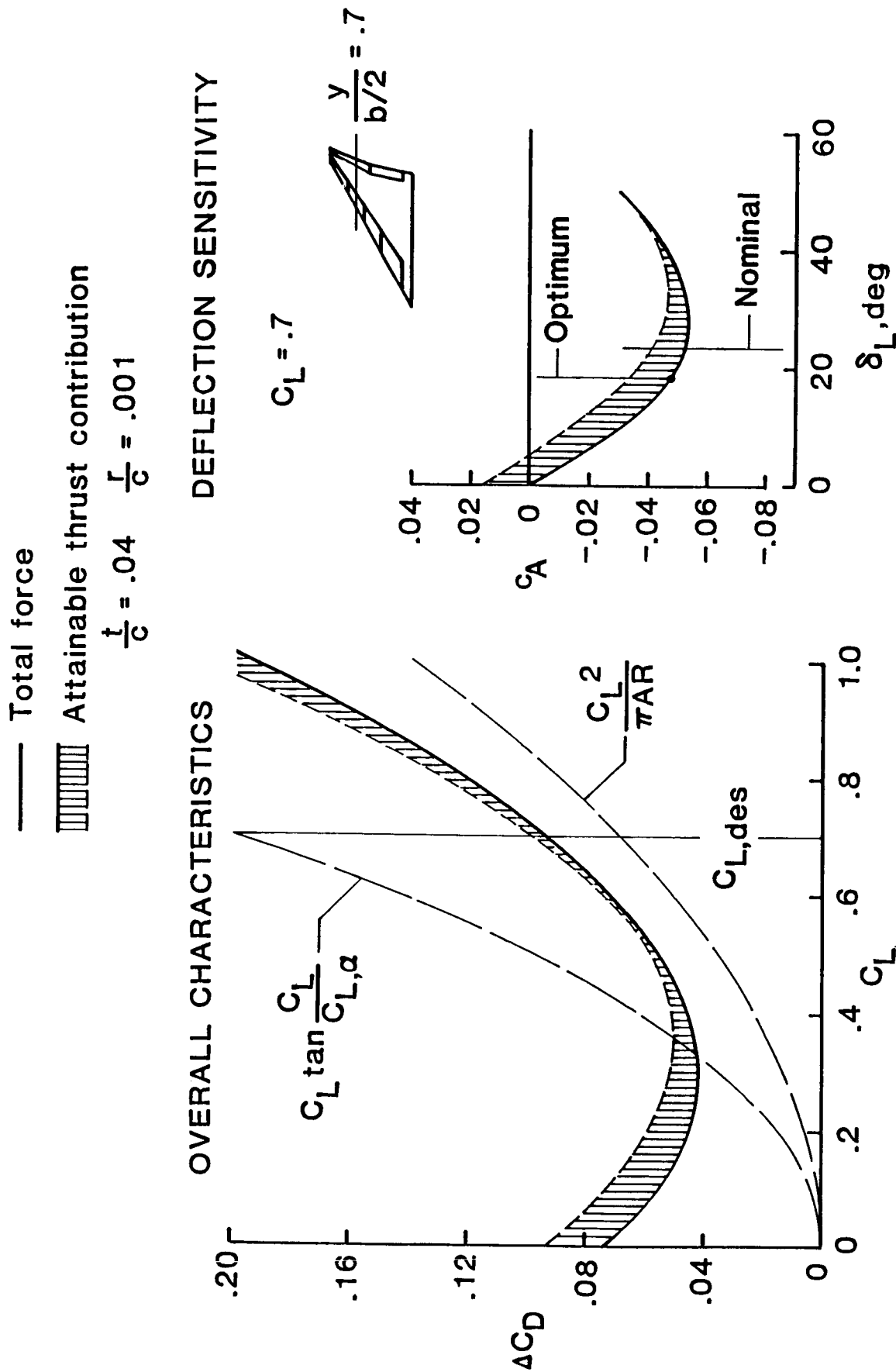R = 2.9 x 10^6, C_L = 0.7.

Figure 11. - Effect of leading edge radius on flap system performance. Sharp leading edge design with rounded leading edge section. M = 0.5, R = 50 x 10^6.

$\frac{y}{b/2}$

.9

.7

.5

.3

.1

$\frac{z}{c_r}$

.1

0

$\frac{z}{c_r}$

0

.1

.2

$\frac{x'}{c_r}$

0 .2 .4 .6 .8 1.0

Camber surface, $\alpha = 0°$

Wing with candidate flaps, $\alpha = -9°$

δ_L, deg

40

20

0
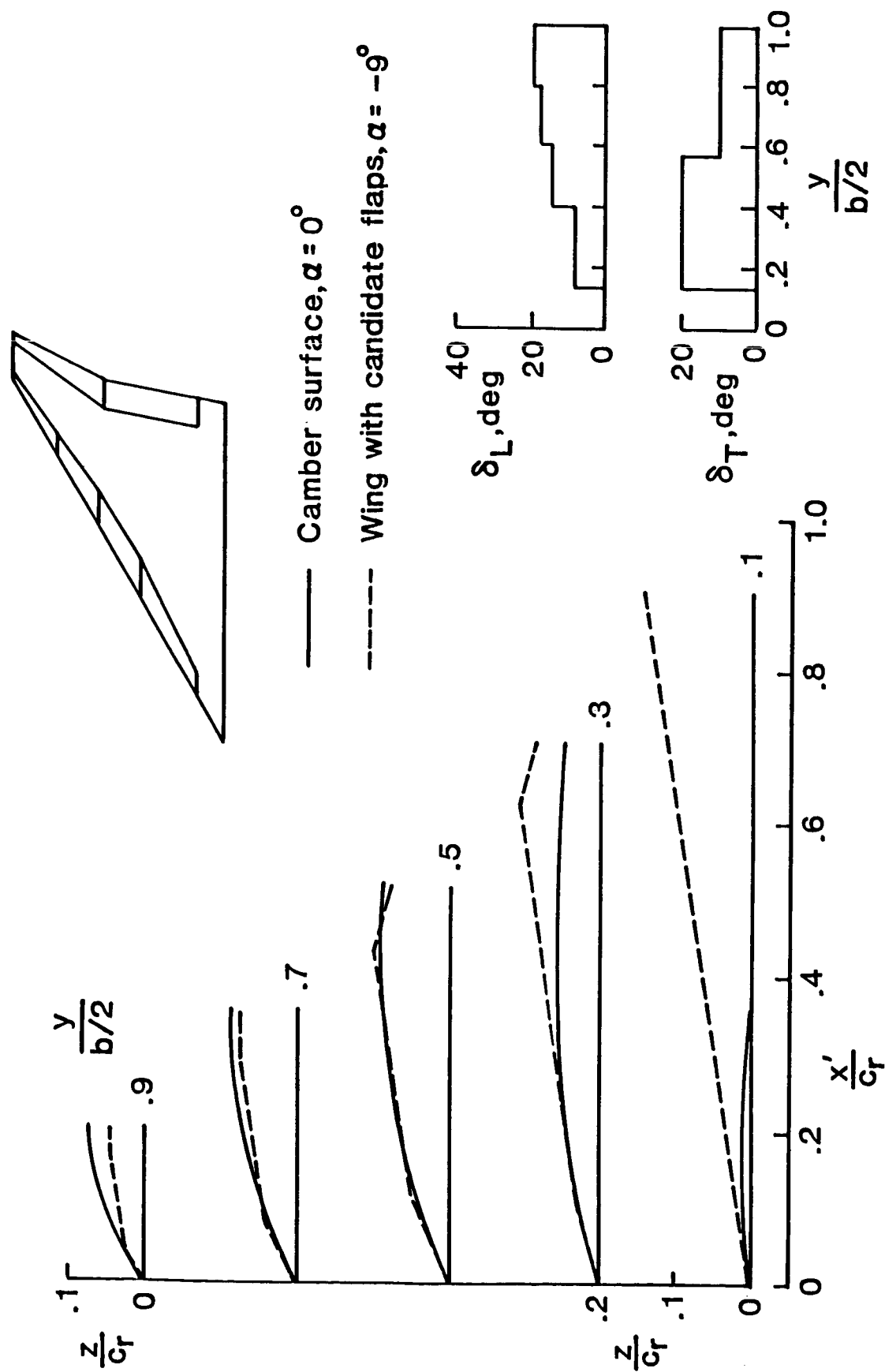
δ_T, deg

20

0

$\frac{y}{b/2}$

0 .2 .4 .6 .8 1.0

Figure 12. - Use of design program for selection of candidate flap system. Whole wing design for a rounded leading edge. M = 0.5, R = 50 x 10^6, C_L = 0.7.
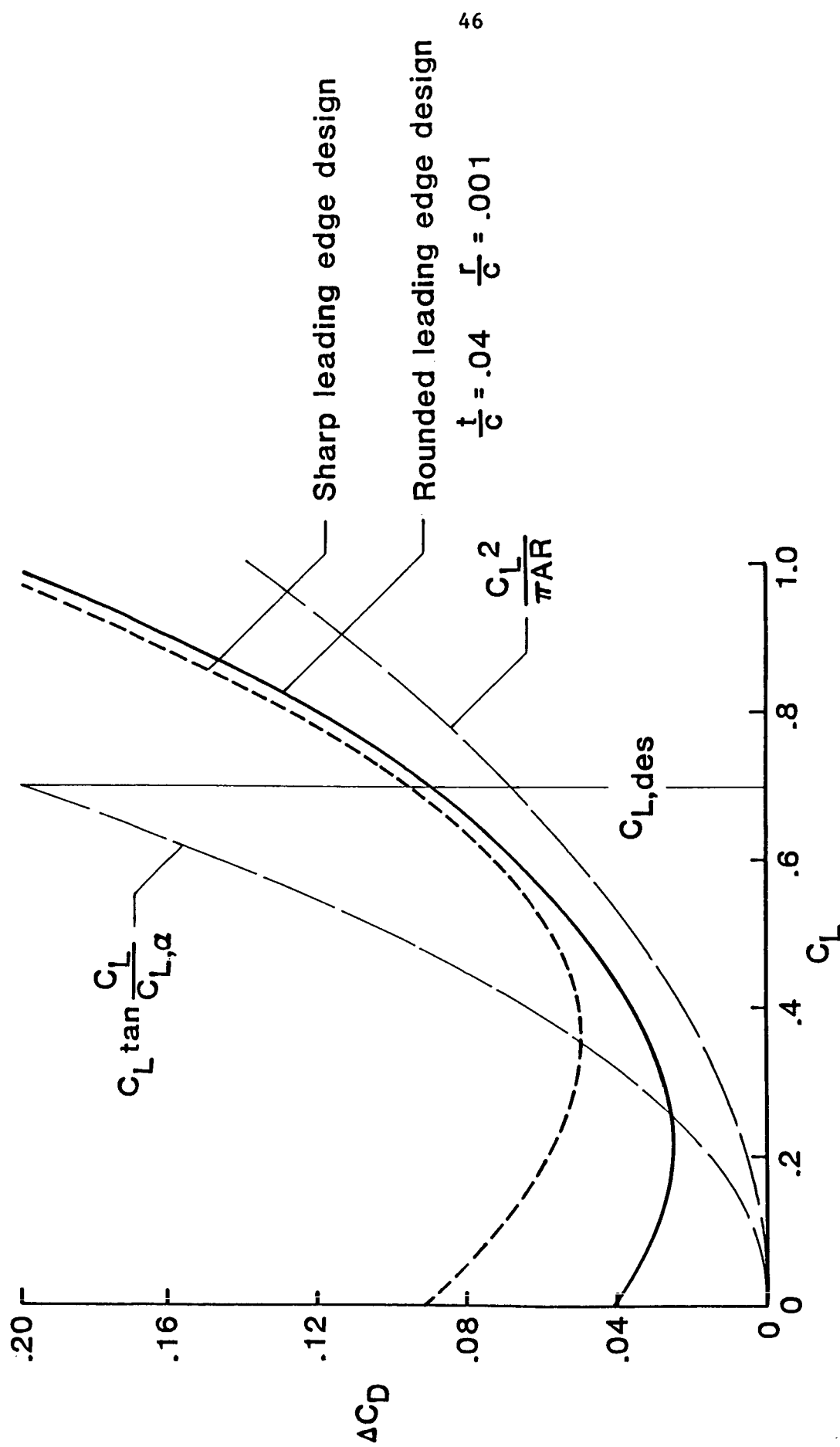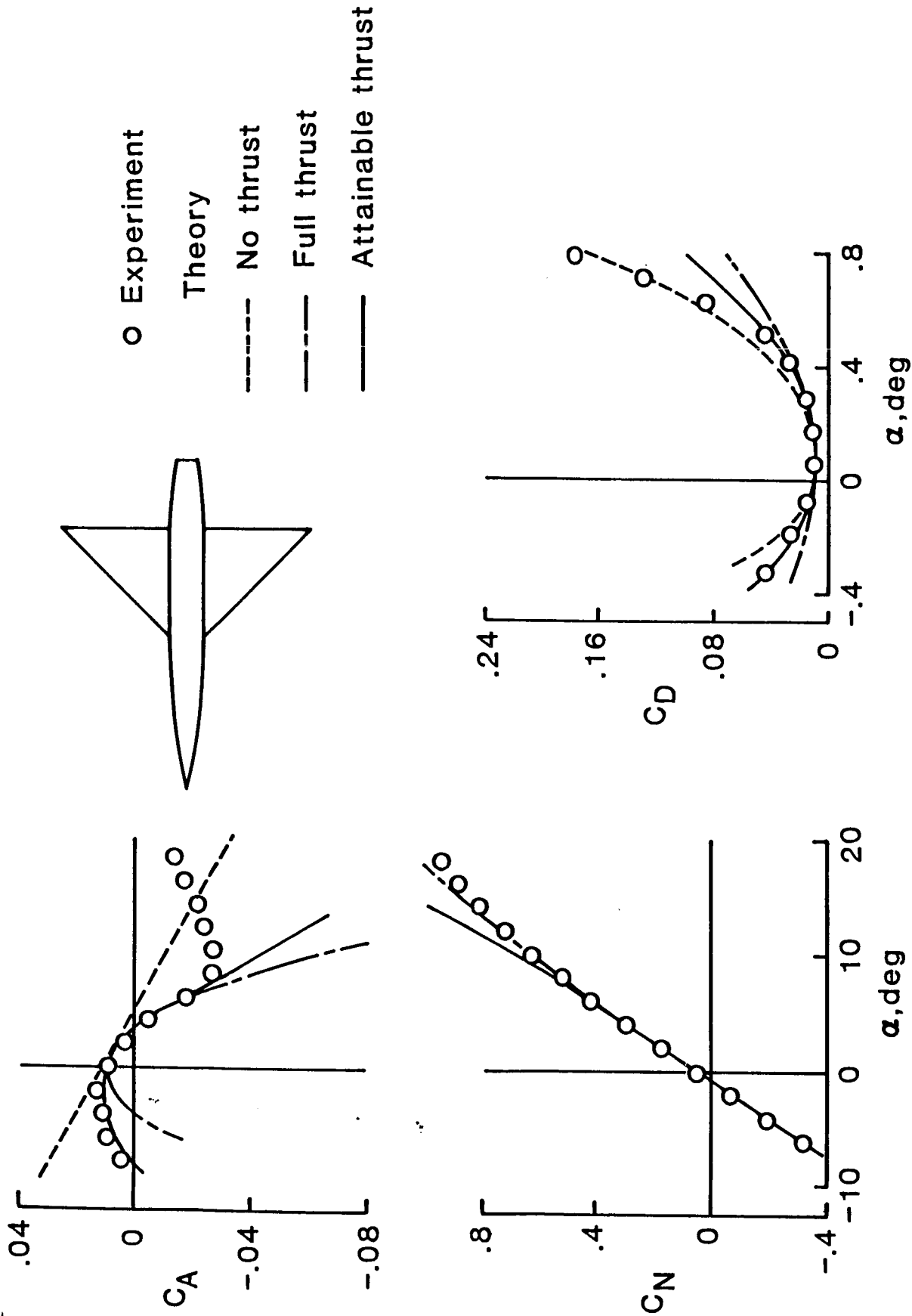
Figure 13. - Comparison of lift-drag characteristics of candidate flap system for sharp and rounded leading edge designs. $M = 0.5$, $R = 50 \times 10^6$.

o Experiment

Theory

------- No thrust

—·—· Full thrust

——— Attainable thrust

Figure 14. - Aerodynamic characteristics at two Reynolds numbers for a twisted and cambered delta wing configuration. M = 0.5.

(a) R = 1.5 x 10⁶

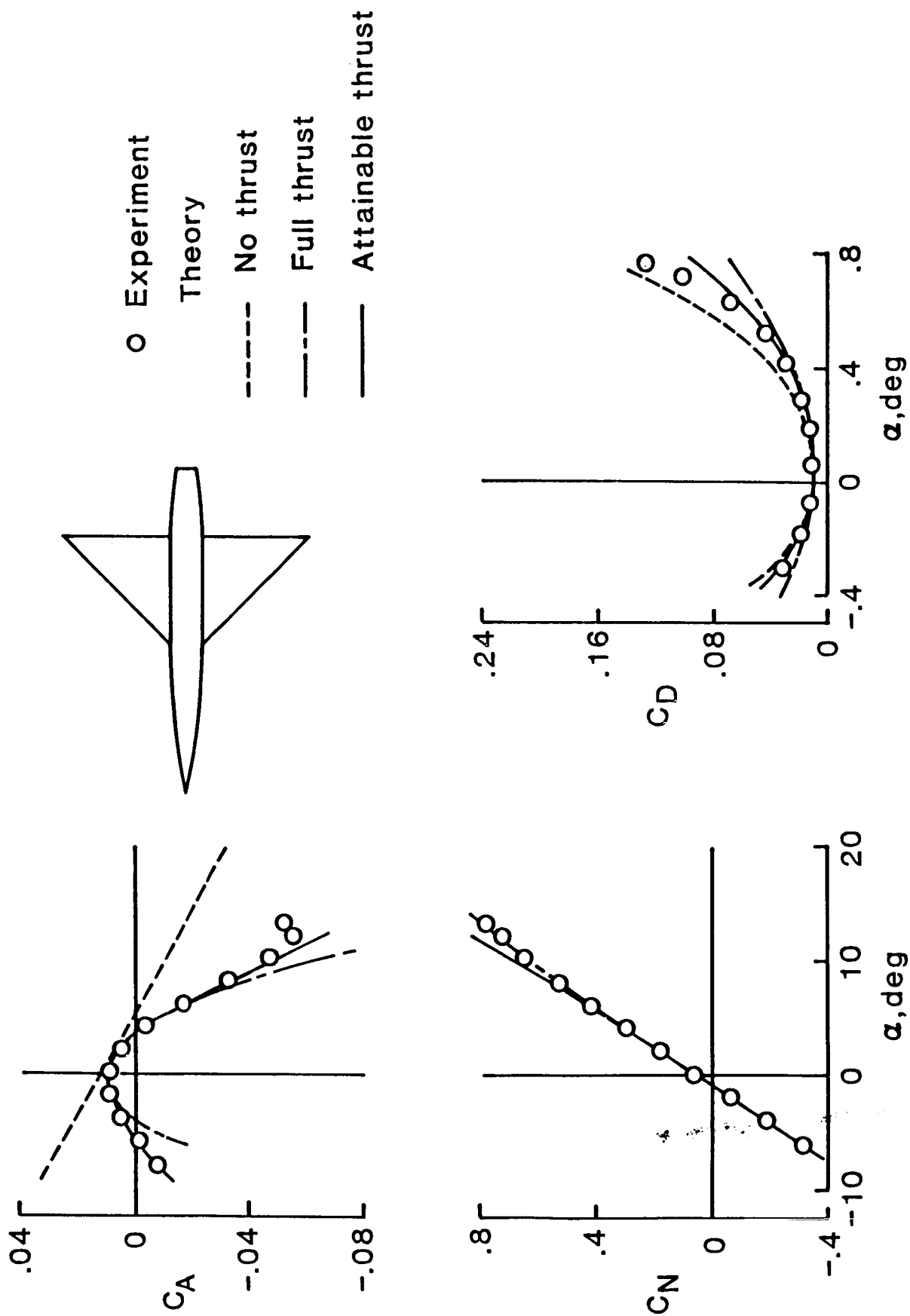o Experiment

Theory

— — — No thrust

— · — Full thrust

———— Attainable thrust

(b) R = 8.0 x 10^6

Figure 14.- Concluded.
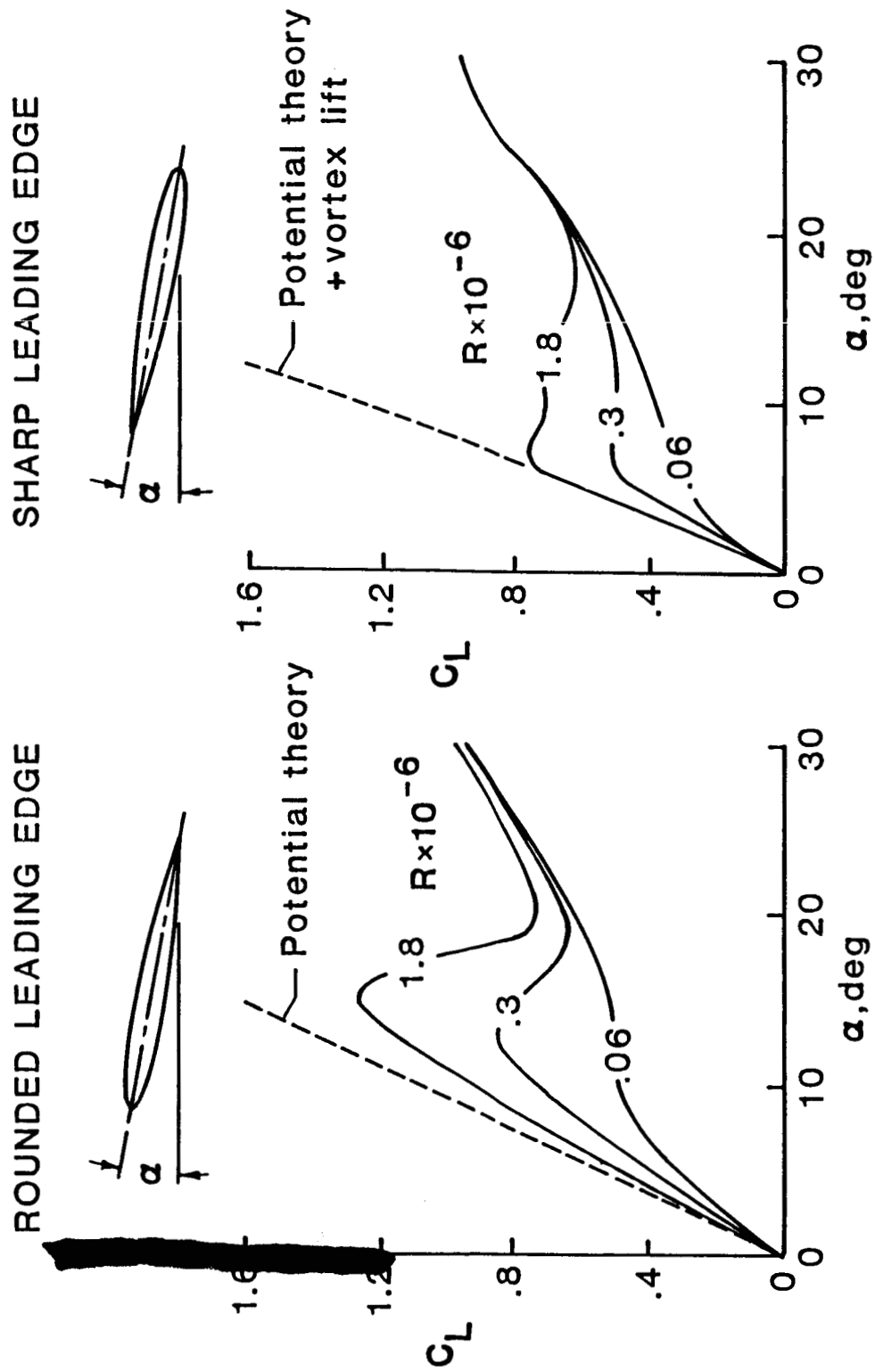
ROUNDED LEADING EDGE

SHARP LEADING EDGE

Figure 15. - Effect of Reynolds number on lift of sharp and rounded
leading edge airfoil sections.

1. Report No. NASA CR-3913	2. Government Accession No.	3. Recipient's Catalog No.
4. Title and Subtitle THE DESIGN AND ANALYSIS OF SIMPLE LOW SPEED FLAP SYSTEMS WITH THE AID OF LINEARIZED THEORY COMPUTER PROGRAMS		5. Report Date August 1985
		6. Performing Organization Code
7. Author(s) Harry W. Carlson		8. Performing Organization Report No.
		10. Work Unit No.
9. Performing Organization Name and Address Kentron International, Incorporated Hampton Technical Center Hampton, VA 23666		
		11. Contract or Grant No. NAS1-16000
		13. Type of Report and Period Covered Contractor Report
12. Sponsoring Agency Name and Address National Aeronautics and Space Administration Washington, DC 20546		
		14. Sponsoring Agency Code 505-43-23-10

15. Supplementary Notes

Langley Technical Monitor: Christine M. Darden

16. Abstract

The purpose of this report is to show how two linearized theory computer programs in combination may be used for the design of low speed wing flap systems capable of high levels of aerodynamic efficiency. A fundamental premise of the study is that high levels of aerodynamic performance for flap systems can be achieved only if the flow about the wing remains predominantly attached. In accordance with this premise, a wing design program is used to provide idealized attached flow camber surfaces from which candidate flap systems may be derived, and, in a following step, a wing evaluation program is used to provide estimates of the aerodynamic performance of the candidate systems. Design strategies and techniques that may be employed are illustrated through a series of examples. Applicability of the numerical methods to the analysis of a representative flap system (although not a system designed by the process described herein) is demonstrated in a comparison with experimental data.

17. Key Words (Suggested by Author(s)) Aerodynamics Numerical methods Wing Design Leading-edge thrust Linearized theory	18. Distribution Statement Until August 1987 Subject Category 02

19. Security Classif. (of this report) Unclassified	20. Security Classif. (of this page) Unclassified	21. No. of Pages 54	22. Price